Finite Element Dynamics of Human Auditory System

Comprising Middle Ear and Cochlea in Inner Ear

Hidayat

June 2017

Summary

The human ear can be divided into three main parts, namely the external ear, the middle ear and the inner ear. The middle ear consists of an eardrum and three ossicles, namely three tiny bones (malleus, incus and stapes) which linked by each other, and connected with the eardrum and the inner ear. The problem in the ear that makes the human being unable to hear sounds in one or both ears is known as hearing loss. Hearing loss is one of the most severe problem in usual life activity of the human being. WHO reports that over 5% of the world's population have hearing loss. Conductive hearing loss is the most common case due to problem in the middle ear or outer ear at times. In the middle ear, conductive hearing loss occurs due to chronic middle ear infection or glue ear where fluids fill up the middle ear so that the eardrum can not move. The otosclerosis in which the ossicles in middle ear become stiff or the dislocation of the three ossicles causes severe conductive hearing loss. The eardrum with a hole also can result in the conductive hearing loss. The eardrum with a hole accompanies liquid discharge from middle ear through the ear canal. Closing the hole in the eardrum can prevent water entering in a middle ear and an ear infection. Conductive hearing loss can often be treated with a surgery using artificial ossicles. The closure of the eardrum with hole by surgery is myringoplasty. If it is possible to perform the simulation of dynamic behavior of the human ear system before the surgery, it must be very helpful.

The purposes of this study are to develop a three-dimensional model of human ear system, to simulate the dynamic behavior of human ear system containing middle ear system, cochlea in inner ear, ligaments, tendon and tensor tympanic membrane and to examine the proper material properties and dimensions of sliced materials used in myringoplasty using finite element analysis (FEA).

The three-dimensional model of human ear system was developed using CAD software (Solidworks 2015) with the shapes and dimensions considering by the other researchers. Then, the three-dimensional model was exported to the finite element analysis software (Hypermesh) to perform dynamic analyses namely eigen-value, frequency response and time history response analyses. Six-node triangular elements and ten-node tetrahedron element were used for the eardrums and the ossicles in finite element analysis, respectively. The material properties of human ear system were defined considering previous published by the other researchers. Three types of boundary conditions, namely clamped, torsional springs and new boundary modeled with finite elements were used on the boundary of the eardrums.

In the dynamic analysis, the eigen-value analyses of the human ear systems and the four types of eardrums, namely a normal eardrum, an eardrum with a hole, an eardrum repaired by the sliced cartilage and the sliced material except cartilage were carried out. Using the eigen-value analysis, it was examined that the proper thicknesses of sliced cartilage were 0.45 [mm] to 0.45 [mm] and sliced material having the same material properties as the human eardrum was 0.1 [mm] by comparing the vibration modes and natural frequencies of the four types of eardrums. Then, the frequency response and time history response analyses of the human ear system had been carried out. In the time history response analysis, Formant frequencies and human voices were used as the frequencies of the external forces and input sound pressures, respectively. It was confirmed that the calculation method in this study can perform dynamics analysis of human ear system containing middle ear, cochlea, ligaments, tendon and tensor tympanic membrane. Predictions from the model in this study may be useful to medical department in researching new surgical reconstruction and provide useful information for the design of prosthesis in the human ear system.

Contents

Chapter 1

Introduction

1.1 Background

Human ear is one of the most complex organ in the human body. The human ear can be divided into three main parts, namely the external ear, the middle ear and the inner ear. The middle ear consist of an eardrum and three ossicles, namely three tiny bones (malleus, incus and stapes) which linked by each other, and connect with the eardrum and the inner ear. Sound waves enter the ear canal and make the eardrum vibrate. This action moves the ossciles (malleus, incus and stapes) in the middle ear. The stapes hit the part of cochlea in inner ear, namely membrane window. Inside the cochlea contains tubes filled with fluid, sensory receptor and nerve receptor for hearing.

The problem in the ear that makes the human being unable to hear sounds in one or both ears is also known as hearing loss. Hearing loss is one of the most severe problem in usual life activity of the human being. WHO reports that over 5% of the world's population have hearing loss. Conductive hearing loss is the most common case due to problem in the middle ear or outer ear at times. In the middle ear, conductive hearing loss occurs due to chronic middle ear infection or glue ear where fluids fill up the middle ear so that the eardrum can not move. The otosclerosis in which the ossicles in middle ear become stiff or the dislocation of the three ossicles causes severe conductive hearing loss. Conductive hearing loss can often be treated with a surgery

using artificial ossicles. If it is possible to perform the simulation of dynamic behavior of the middle ear before the surgery using artificial ossicles, it must be very helpful.

In the human middle ear, an eardrum with a hole can result in the conductive hearing loss. The eardrum with a hole is also known as eardrum perforation. Eardrum perforation accompanies liquid discharge from middle ear through the ear canal. The hole in eardrum can be caused by an ear infection, an injury to the eardrum such as poking an object like a cotton bud into the ear, changes in air pressure such as the diving and a sudden load noise such as explosion. Closing the hole in an eardrum can prevent water entering in a middle ear and an ear infection. The closure of the eardrum with hole by surgery is myringoplasty. A sliced cartilage is generally used for myringoplasty. The cartilage can be easily obtained from inside of the external ear.

Based on this background, the main subject of this research are modeling the three dimensional model and simulation dynamic behavior of human ear system using finite element method. The shape, dimension and material properties of the human ear system were defined using the previous published by the other researchers. Then, the eigen-value, frequency response and time history response analyses were performed to simulate the dynamic behavior of human ear system.

1.2 Literature Review

A review of published papers dealing with the studies on finite element dynamics of human ear system containing middle ear, cochlea in inner ear, ligaments, tendon and tensor tympanic membrane is presented in this section. The papers were reviewed based on the purposes of this research. The summary of the literature review is shown in Fig. 1.1.

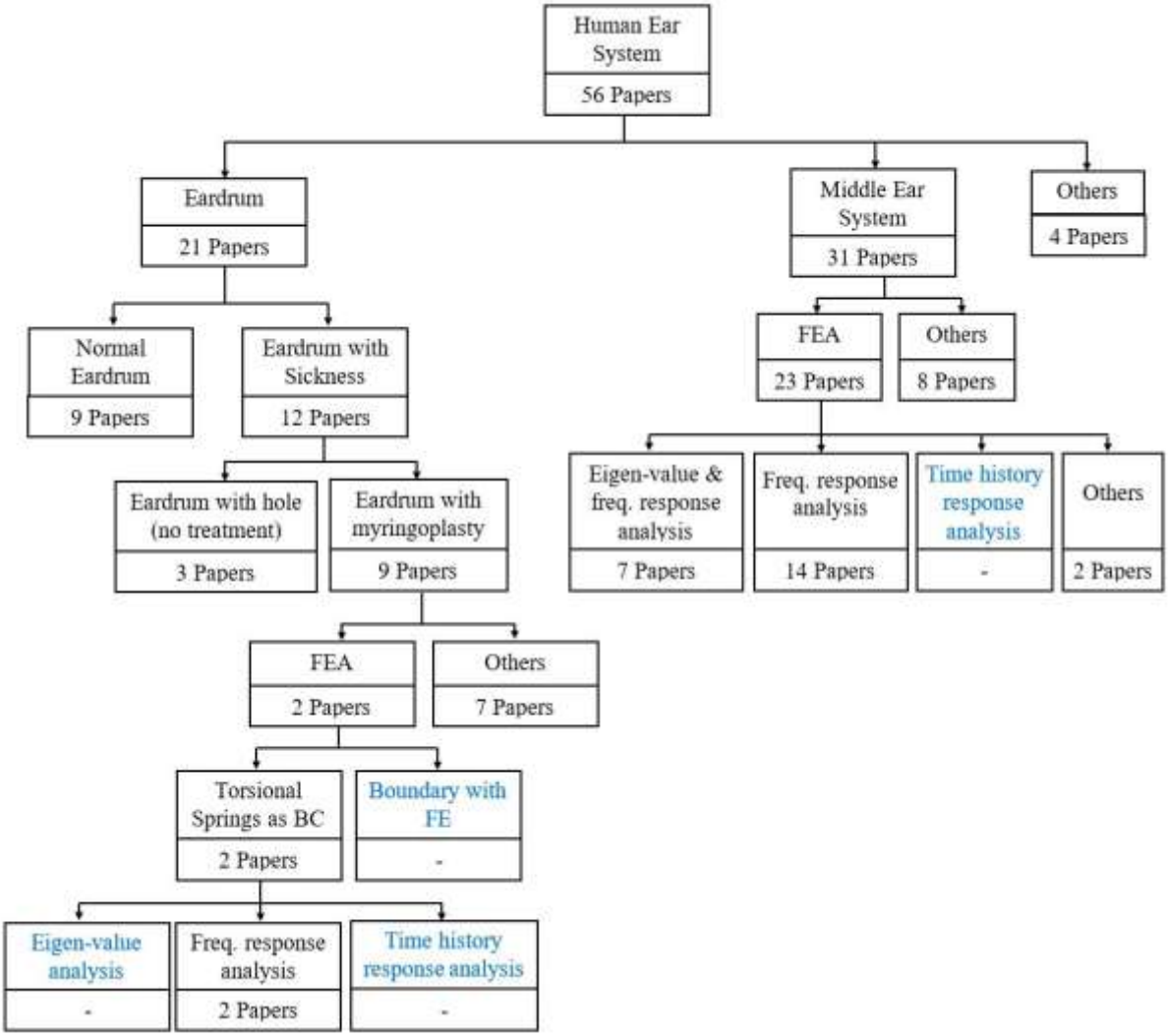

Fig. 1.1 Summary of the literature review

There are 56 [1 – 56] papers discussed about human ear system reached by the author. As far as the author reached, there are 21 paper [1-21] reported on only eardrums. The 9 papers [1 – 9] reported on normal eardrum and the 12 papers [10 – 21] discussed about eardrum with sickness, in this case, there is a hole on the surface of the eardrum. As for the eardrum with a hole, there are 3 papers [10-12] reported the hearing ability of human using eardrum with hole and there are 9 papers [13-21] discussed about the closure of eardrum by using cartilage as graft material. There are only 2 papers [20 – 21] reported the use of cartilage in myringoplasty using finite element analysis. Lee et.

al determined the characteristics of cartilage for optimal cartilage myringoplasty [20] and the optimal graft thickness for cartilage myringoplasty with different sizes of tympanic membrane [21]. As far as the author reached, there is no paper performing time history response and eigen-value analysis to simulate the dynamic behavior of eardrum with myringoplasty.

Then, the 31 papers [22 – 52] reported on human ear system consisting of middle ear system, ligaments, tendon and tensor tympanic membrane. There are 23 papers [22 – 44] performing simulation using finite element analysis. Then, the 7 papers [22- 28] performed eigen-value and frequency response analysis. There are 14 papers [29 – 42] performing only frequency response analysis.

As far as the authors reached, there is no report performing time history response analysis using Formant frequencies as the external forces and human voices as the input sound pressures as presented in this study.

1.3 Purposes of Research

The purposes of this research are listed as follows

1. To make the three-dimensional model of the human ear system using CAD software.
2. To simulate the dynamic behavior of the human ear system comprising the middle ear, cochlea in inner ear, ligaments, tendon and tensor tympanic membrane using finite element method.
3. To examine the proper material properties and dimensions of sliced materials used in myringoplasty of humans using finite element method.

1.4 Description of Dissertation

The dissertation is described in the following manner. Chapter 1 presents the background, literature review, purposes of the research and description of the dissertation. The literature review is addressed to the dynamics analyses of the human ear system using finite element method.

Chapter 2 presents a study on 3D modeling of the human ear system. The human ear system is composed of the middle ear system, cochlea in inner ear, ligaments, tendons and tensor tympanic membrane. Then, the middle ear system consists of the eardrum and the three ossicles namely malleus, incus and stapes. The eardrum with flat shape and the human eardrum with concave shape as analysis models is presented. The clamped boundary condition on the boundary of the flat eardrum is presented. Then, the clamped boundary condition and torsional spring were applied to the concave eardrum. In this chapter, the eardrum with sliced materials used in myringoplasty was presented. Four types of the eardrum namely normal eardrum, eardrum with a hole, eardrum repaired by sliced cartilage and materials is developed in this step. Then, the 3D model of three ossicles, cochlea in inner ear, ligaments, tendons and tensor tympanic membrane were created.

Chapter 3 presents a study of dynamics analyses of the human eardrum using finite element method. The eigenvalue analysis, frequency response analysis and time history response analysis for the human eardrum are presented. The eigenvalue analysis and frequency response analysis to simulate the dynamic behavior of the human eardrum with flat shape and concave shape using finite element method are presented. Then, the eigenvalue analysis for the eardrum with sliced materials used in myringoplasty to compare the natural frequency and vibration modes to the normal eardrum is presented.

Chapter 4 presents a study of finite element dynamics of human ear system. The eigenvalue, frequency response and time history response analysis was performed for human ear system using torsional spring as boundary conditions. Then, the time history response analysis using formant frequency on the external forces and human voices as the external forces is presented. The human ear system using boundary modeled with finite elements considering the four types of the eardrums are presented.

Finally, chapter 5 presents conclusions of the research. In additions list of reference of reviewed literature and publications as the core of dissertation are given at the end of this dissertations.

Chapter 2

3D Modeling of Human Ear System

2.1 Introduction

The purpose of the study presented in this chapter is to develop a 3D modeling of human ear system. The geometric models on human ear system were generated by the CAD software (Solidworks 2015) using the physical properties of components of the human ear system reported by the other researchers.

The analysis model of human ear system used in this chapter is composed of the middle ear system, cochlea in inner ear, ligaments, tendon and tensor tympanic membrane. Then, the middle ear system consists of an eardrum and three ossicles (malleus, incus and stapes). As for the eardrum, the eardrum with flat shape and the human eardrum with concave shape are presented. The clamped boundary conditions was used on boundary of eardrum with flat shape. Two types of boundary conditions namely clamped and torsional spring are presented on boundary of human eardrum with concave shape. The next step in this study, the eardrum with sliced materials used in myringoplasty is also presented. Then, four types of the 3D models of the eardrums

namely normal eardrum, eardrum with a hole, eardrum repaired by the sliced cartilage and the sliced material having the same material properties as the human eardrum are develoed. The new boundary modeled with finite elements are presented for the four types of the eardrum. Finally, the 3D modelling of the human ear system comprising the middle ear system, cochlea in inner ear, ligaments, tendon, and tensor tympanic membrane were developed.

2.2 Middle Ear System

2.2.1 Flat Eardrum (Eardrum with Flat Shape)

2.2.1.1 Analysis Model of Flat Eardrum

Figure 2.1 shows the shape and dimensions of flat eardrum. As for the dimensions of the flat eardrum, the values of 10.0 [mm], 9.0 [mm] and 0.1 [mm] were used as the major axis, the minor one and the thickness, respectively by considering those reported by other researchers [3]. The shape and dimension of flat eardrum was made by using CAD software (Solidworks 2015). Then, the shape and dimension were exported to the Hypermesh as IGS file.

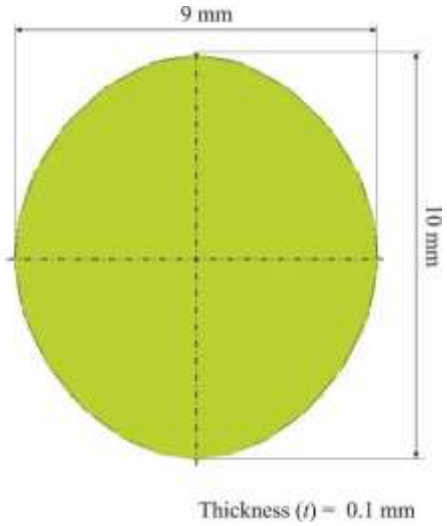

Fig. 2.1 Shape and dimensions of flat eardrum

In the Hypermesh software, the shape and dimension were meshed by using two types of elements, namely three-node triangular element and six-node triangular element. Figure 2.3 show the three-node element (low order element). In this element, there are three node at the each corner of triangle shape. The triangular element with three-node is also known as low order element.

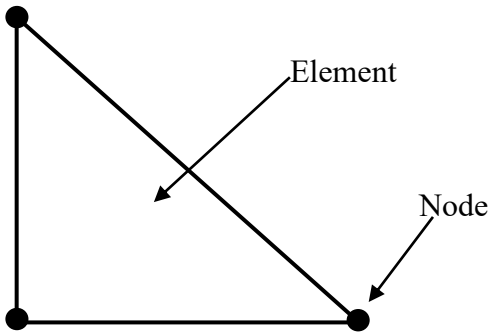

Fig. 2.3 Three-node triangular element (low order element)

Figure 2.4 shows the six-node triangular element (high order element). The six-node triangular element was used for flat eardrum to perform eigen-value analysis and frequency response analysis. The six-node triangular element is also known as high order element.

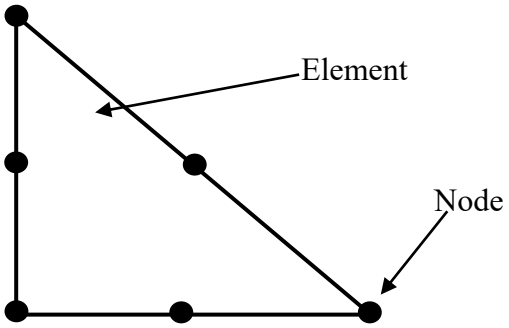

Fig. 2.4 Six-node triangular element (high order element)

Figure 2.4 shows the finite element model of flat eardrum meshed by triangular element. The three-node and six-node triangular element were investigated in this analysis model using eigen-value and frequency response analysis. The comparison of the usage of three-node triangular element and six-node triangular will be carried out in this study.

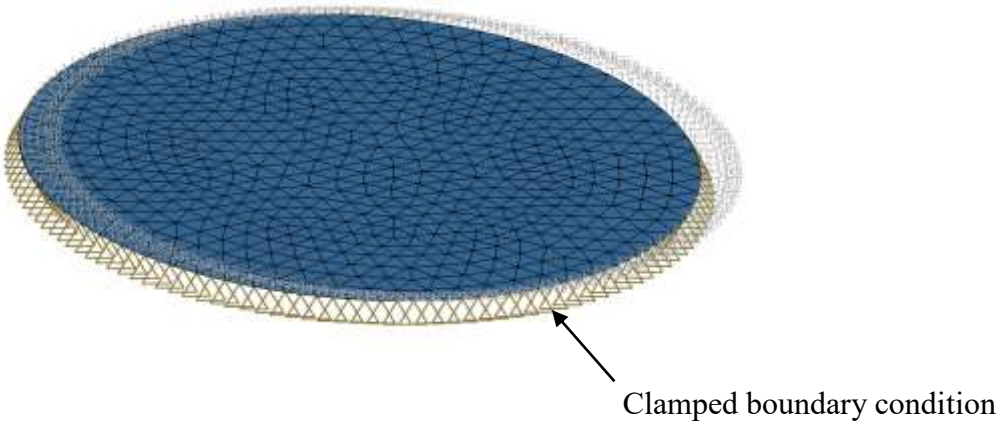

Fig. 2.4 Finite element model of flat eardrum meshed by triangular element

Figure 2.5 shows the clamped boundary condition applied on the boundary of eardrum. In this study, clamped boundary condition is one of the boundary of the eardrum used to perform dynamics analysis of the human eardrum using finite element method.

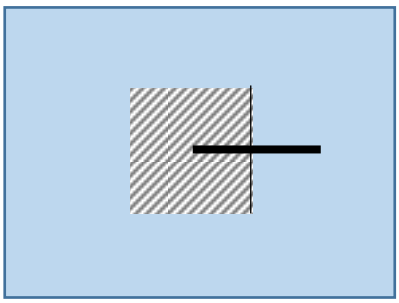

Fig. 2.5 Clamped boundary condition applied on the boundary of eardrum

2.2.1.2 Examination of Proper Type and Number of Finite Elements on Flat Eardrum

Proper type and partition number of finite elements on flat eardrum were examined. Three-node and six-node triangular elements were used as finite elements. As for the material properties of an eardrum, the values of 33.4 [MPa], 1.2×10^3 [kg/m^3] and 0.3 were used as the Young's modulus, the mass density and the Poisson's ratio respectively by considering those reported by other researcher [22]. Then frequency response analyses were carried out for flat eardrum with the clamped boundary condition using the HyperMesh (Finite Element Analysis (FEA) code).

Figure 2.6 shows the partition number of finite elements affecting natural frequencies of flat eardrum with the clamped boundary condition. As for flat eardrum, there are six natural frequencies less than 1,500 [Hz]. Then the displacements of natural frequencies over 1,500 [Hz] become very small because a large value is used as the structural damping coefficient over 1,500 [Hz]. The FEA solutions, namely numerical solutions of natural frequencies are approaching to the analytical ones, namely exact one as the number of finite elements become larger. The FEA solutions on natural frequencies hardly vary over 1,000 elements. It is also well known that the computational precision is not good for two-dimensional three-node triangular element and three-dimensional four-node tetrahedron one because a strain becomes constant inside those elements. Therefore, it was decided to divide the flat eardrum into 1,274 elements using the six-node triangular one in this research.

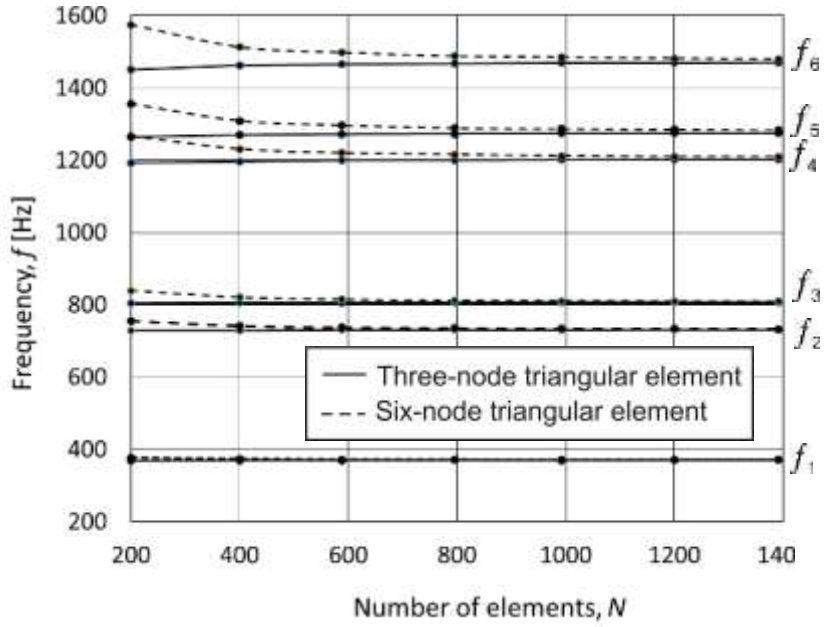

f_i (i = 1 ~ 6) : Natural frequency

Fig. 2.6 Partition number of finite elements affecting natural frequencies on flat eardrum with the clamped boundary condition.

2.2.2 Concave Eardrum (Human Eardrum with Concave Shape)

2.2.2.1 Analysis Model of Concave Eardrum

Figure 2.7 shows the shape and dimensions of concave eardrum created by CAD software. The shape of concave eardrum was created by using CAD software (Solidworks 2015). Then, as for the major and minor axes of concave eardrum, the same values as flat eardrum were used. For the height of the concave shape of concave eardrum, the value of 1.5 [mm] was used considering by the other researcher [22]. The concave shape of eardrum was exported to the Hypermesh as a IGS file.

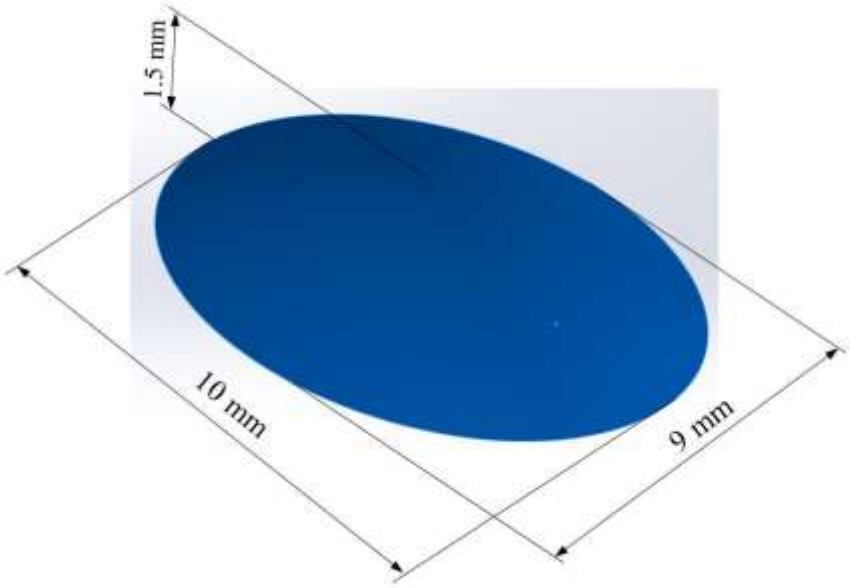

Fig. 2.7 Shape and dimensions of concave eardrum created by CAD software

Figure 2.8 shows the analysis model of concave eardrum. The concave shape of eardrum was exported to the Hypermesh as an IGS file. In the Hypermesh, the shape of concave eardrum were meshed using six-node triangular elements. For all material properties of the concave eardrum, namely the Young's modulus, the mass density and the Poisson's ratio, the same values as flat eardrum were used.

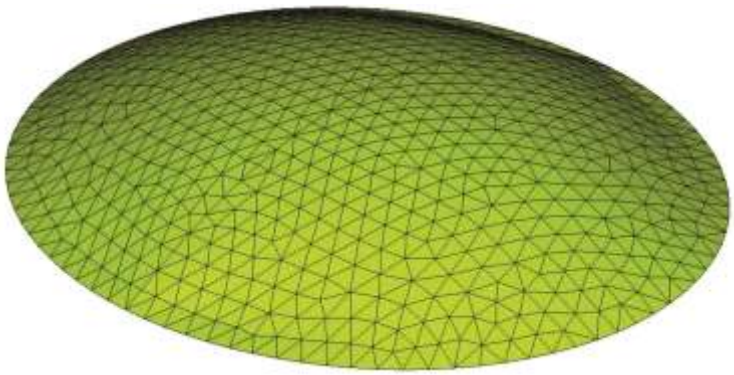

Fig. 2.8 Analysis model of concave eardrum

2.2.2.2 Concave Eardrum Using Clamped Boundary Conditions

Figure 2.4 show the finite element model of concave eardrum that is divided by 1,220 pieces of six node triangular elements using clamped boundary conditions. The boundary of the eardrum were fixed for all degrees of freedom.

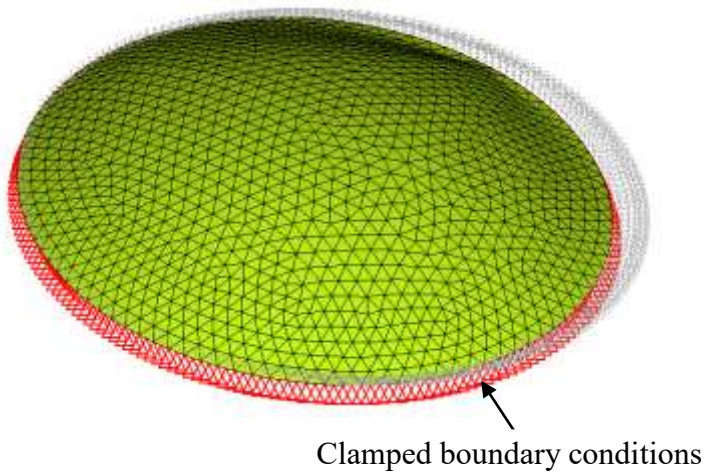

Fig. 2.4 Finite element model of concave eardrum that is divided by 1,220 pieces of six-node triangular elements using clamped boundary conditions

2.2.2.3 Concave Eardrum Using Torsional Spring as Boundary Conditions

Figure 2.5 shows the finite element model of concave eardrum using torsional springs as boundary conditions that is divided by 1,220 pieces of six-node triangular elements. The dimensions and the material properties of the concave eardrum using torsional springs as boundary conditions are the same ones as those of the eardrum using clamped boundary conditions. Each node at boundary of the eardrum using torsional spring as boundary conditions has its own local coordinate frame. In the local coordinate frame, three translational motions in the x-, y, and z-direction and two rotational ones around the x-, y-, and z-axis were fixed. Then the torsional springs were applied at the nodes on boundary of the concave eardrum. The torsional springs were used to

control the stiffness of boundary conditions in order to make the concave eardrum using torsional springs as boundary conditions similar to a real human eardrum.

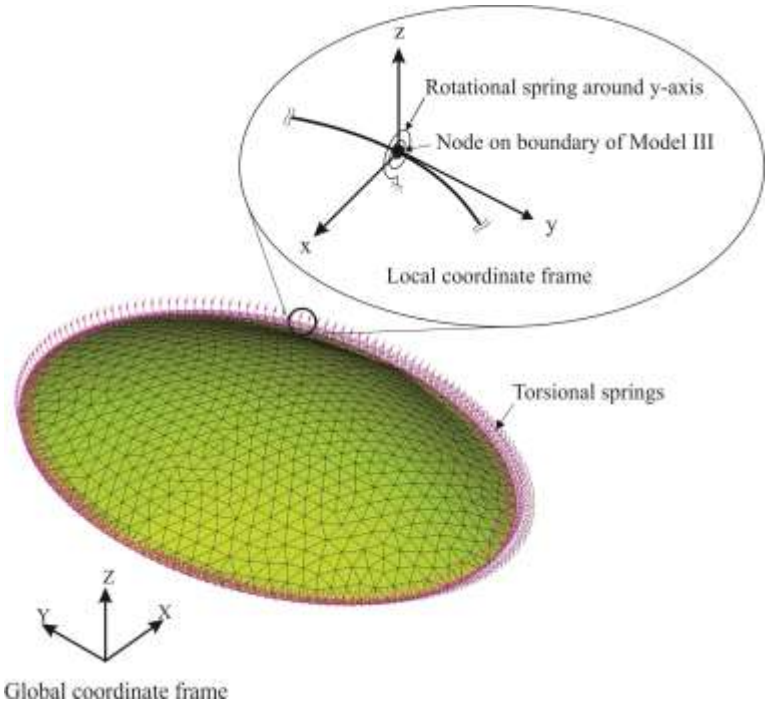

Fig. 2.5 Finite element model of the concave eardrum using torsional springs as boundary conditions that is divided by 1,220 pieces of six-node triangular elements

2.2.3.2 Validation of Torsional Springs Used as Boundary Conditions

The eigenvalue analyses were carried out for the concave eardrum with torsional springs as boundary conditions using the HyperMesh (Finite Element Analysis (FEA) code). Figure 2.6 shows the torsional spring constants affecting natural frequencies of the concave eardrum using torsional springs as boundary conditions. The various torsional spring constants were used in the range from $K = 0$ to $K = 100$ [Nmm/rad] for the first six natural frequencies of the concave eardrum. The least square method was used to make approximate curves. It can be seen that the first six natural frequencies become constant in $K = 0.1$ [Nmm/rad] and more.

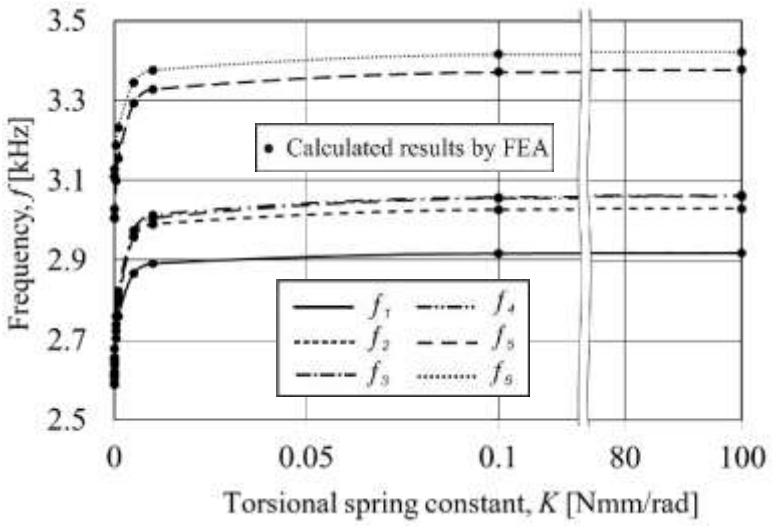

Fig. 2.6 Torsional spring constants affecting natural frequencies of the concave eardrum using torsional springs as boundary conditions

2.2.3 Eardrum with Sliced Materials used in Myringoplasty

2.2.3.1 Modeling of Boundary of Eardrum Using Finite Elements

Figure 2.7 shows the rotational springs element as boundary condition were used for the eardrum with flat shape and the concave shape. In the rotational springs element as boundary conditions, a local coordinate frame was defined for each rotational spring element at a node on boundary of the eardrum. In each local coordinate frame, three translational motions in the *x*-, *y*- and *z*- directions and two rotational ones around the *x*-, and *z*- axes were clamped. As for the rotational spring constant around the *y*-axis, the same value, $K_{\theta y} = 3.0 \times 10^{-5}$ [Nmm/rad] as the authors' previous reports was used so that the boundary conditions of an analysis model of an eardrum can become similar to those of a human eardrum.

Fig. 2.7 Boundary modeled with rotational spring elements

In order to make the modeling of boundary of an eardrum more simple, the new boundary modeled with finite elements having the same dynamics behavior as the boundary modeled with the torsional springs was proposed. Three types of boundary of an eardrum were investigated. The three types of boundary were adjusted in three angles to the horizontal, namely 0 degree, 90 degrees and 45 degrees. The boundary modeled with finite elements using angles 0 degree, 90 degrees and 45 degrees to the horizontal were defined as Model I, Model II and Model III, respectively. Fig. 2.8 Boundary modeled with finite elements defined as Model I. In this boundary model, the finite elements have the same thickness, t = 0.1 [mm] as the human eardrum. The boundary was adjusted 0 degree (parallel) to the horizontal.

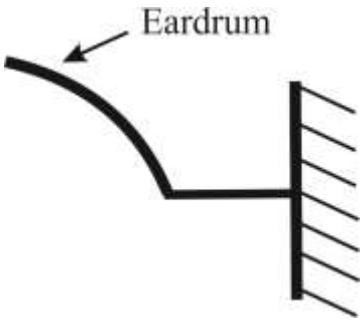

Fig. 2.8 Boundary modeled with finite elements defined as Model I

Figure 2.9 show the boundary modeled with finite element defined as Model II. In this model, the angle of boundary modeled with finite elements was adjusted 90 degrees to the horizontal. Then, the thickness of boundary, the finite elements have thickness the same as the human eardrum.

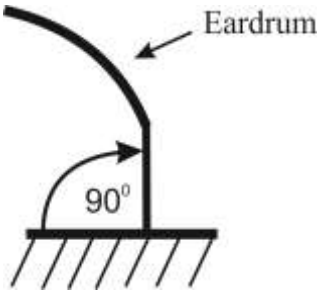

Fig. 2.9 Boundary modeled with finite elements defined as Model II

Figure 2.10 shows the boundary modeled with finite elements. The angle of boundary modeled with finite elements were adjusted 45 degrees to the horizontal. The finite elements have the same thickness, t = 0.1 [mm] as the eardrum. The bottom and other sides of boundary modeled with finite elements were clamped and connected to finite elements of an eardrum, respectively. All boundary modeled with finite elements were divided by 204 pieces of six-node triangular elements. As for material properties of the boundary modeled with finite elements, the same mass density and Poisson's ratio as those of an eardrum were used. Then, the Young's modulus was decided by trial and error considering mode shapes and natural frequencies of the boundary modeled with rotational springs elements.

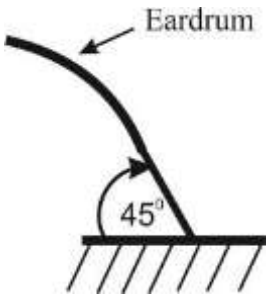

Fig. 2.10 Boundary modeled with finite elements defined as Model III

The eigenvalue analysis was used to examine the Young's modulus for all model of boundary modeled with finite elements considering the vibration modes and natural

frequencies of the boundary modeled with rotational springs elements. The value of E = 491.1 [× 10^6 N/m^2], 817.7 [× 10^6 N/m^2] and 319.3 [× 10^6 N/m^2] was obtained as the Young's modulus of the Model I, Model II and Model III, respectively by using trial and error method. Then, the Model III with value of Young's modulus, E = 319.3 [× 10^6 N/m^2] was defined as the boundary of eardrum modeled with finite elements due to the lowest Young's modulus of the material properties. Then, the boundary modeled with finite element defined as Model III were used for all analysis model in the next steps.

2.2.3.2 Normal Eardrum

Figure 2.8 shows the finite element model of a normal eardrum. The finite element model of a normal eardrum was meshed by 2,150 pieces of the six-node triangular elements. The material properties of an eardrum are shown in Table 1. As for the material properties of eardrum, the same values used in the author's previous report were used. As for the boundary condition of the normal eardrum, the boundary modeled with finite elements was used.

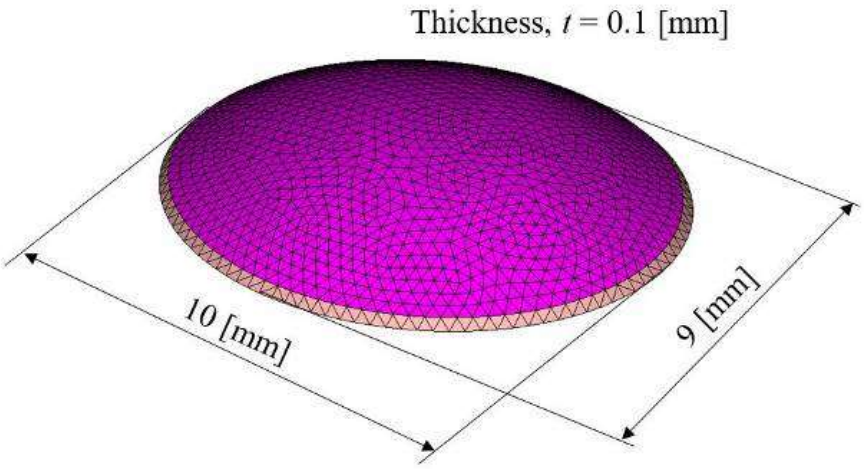

Fig. 2.8 Finite element model of the normal eardrum

Table 1. Material properties of eardrum and cartilage

Materials	Young's modulus [$\times 10^6$ N/m^2]	Mass density [$\times 10^3$ kg/m^3]	Poisson's ratio [-]*
Eardrum	33	1.2	0.3
Cartilage	2.8	1.3	0.3

*[-] means a dimensionless quantity

2.2.3.3 Eardrum with a Hole

The eardrum with a hole causes often the problem called a conductive hearing loss. Figure 2.9 shows the finite element model of the eardrum with a hole. The hole with diameter, D = 2.5 [mm] was located between the center and the boundary of the eardrum. This finite element model was used to examine the effect of the eardrum with a hole to the hearing ability of a human.

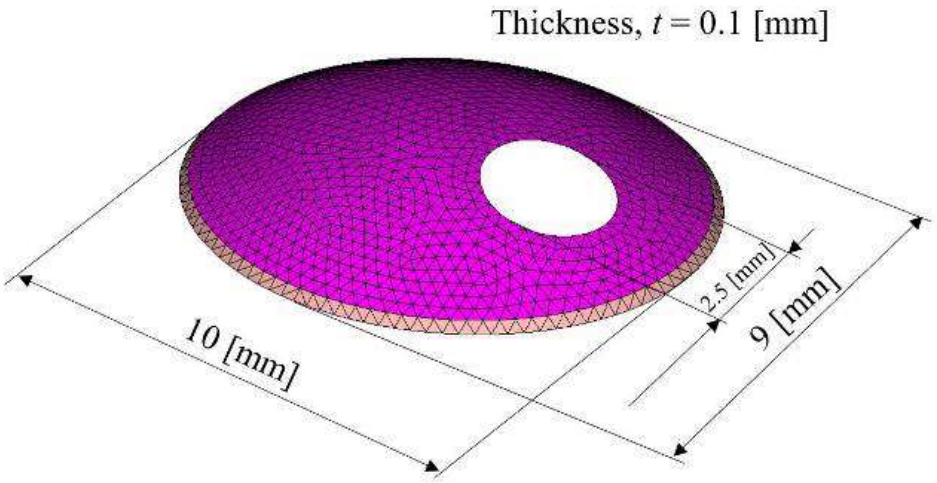

Fig. 2.9 Finite element model of the eardrum with the hole

2.2.3.4 Eardrum Repaired by Sliced Cartilage

Figure 2.10 shows the finite element model of the eardrum repaired by sliced cartilage. As for the diameter of sliced cartilage, the value of D = 2,5 (or 2.7) [mm] was used. Then, as for the thicknesses (or thickness), t of the sliced cartilage, the values from 0.02 [mm] to 0.5 [mm] were used. Then, the sliced cartilage was meshed by the six-node triangular elements. The material properties of sliced cartilage are shown in Table1.

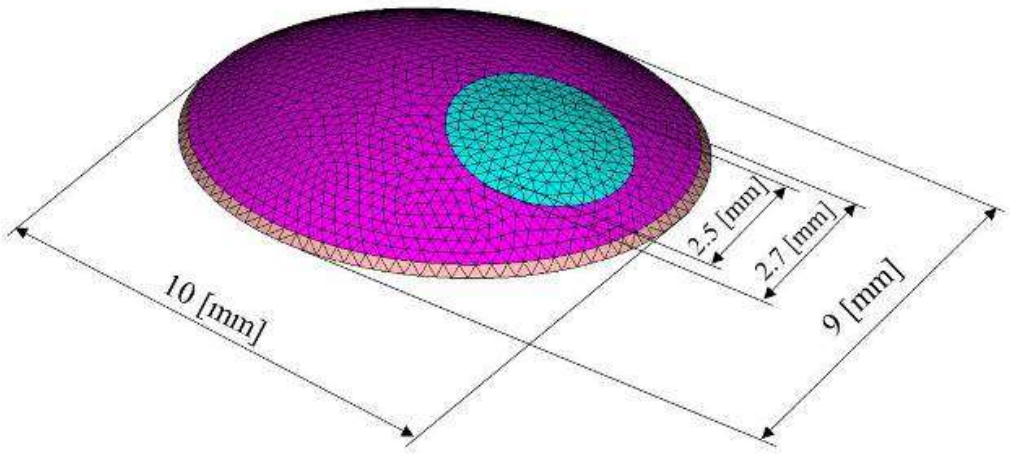

Fig. 2.10 Finite element model of the eardrum repaired by the sliced cartilage or the sliced material

2.2.3.5 Eardrum Repaired by Sliced Materials except Cartilage

Figure 2.10 shows the finite element model of the eardrum repaired by sliced material except cartilage. In this section, the sliced material having the same material properties as the human eardrum was used. As for the dimension of the sliced material, the same diameter as the sliced cartilage was used. Then, the thicknesses of the sliced material from t = 0.02 [mm] to 0.5 [mm] were used.

2.2.4 Three Ossicles (Malleus, Incus and Stapes)

The ossicles are consists of three bones located in the human middle ear that are among the smallest bones in the human body. When the eardrum vibrates as sound hits its surface, it sets the ossicles into motion. The ossicles are arranged in a special order to perform their job. A tendon, tensor tympanic membrane and some ligaments namely superior malleal ligament, posterior incudal ligament, lateral malleal ligament, anterior malleal ligament were attached to the ossicles. The movements of the ossicles is controlled by the ligaments, tendon and tensor tympanic membrane.

Figure 2.11 shows the finite element model of the malleus. The malleus is directly behind and connected to the eardrum. The malleus also known as the hammer. A large sound was collected by the hammer. The hammer is arranged so that one end attached to the eardrum and the other side of the hammer connected to the incus.

Fig. 2.11 Finite element model of the malleus

Figure 2.12 shows the finite element model of the incus. The incus lays at the center of the three ossicles connected to the malleus and the stapes. The incus shapes like an anvil so that the incus is also know as the anvil. The incus forms a lever with the

malleus thereby amplifying incoming sound and aiding in the impedance function of the middle ear.

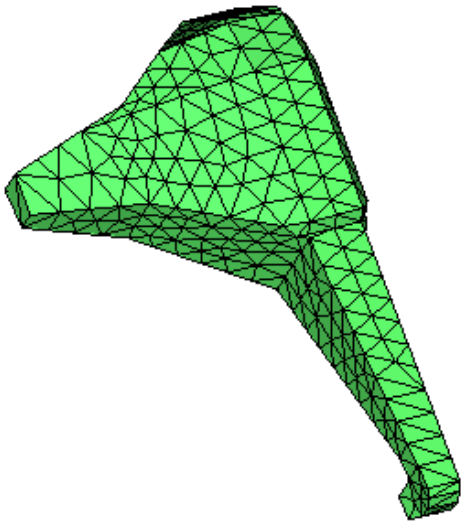

Fig. 2.12 Finite element model of the incus

Figure 2.13 the finite element model of the stapes. The stapes is the smallest and lightest bone in the human body located between the incus and the inner ear. The stapes is a bone in the middle ear of humans involved in the conduction of the sound vibration to the inner ear.

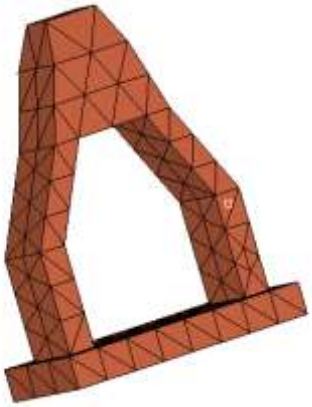

Fig. 2.13 Finite element model of the stapes

2.3 Cochlea in Inner Ear

A cochlea is a part of an inner ear. The cochlea has a snail-like shape and is filled with fluid. There are tiny hair cells as a sensory receptor inside the cochlea. Two are canals for transmission of pressure and in the third is the sensitive organ of Corti, which detects pressure impulses and responds with the electrical impulses which travel along the auditory nerve to the brain. The stapes, namely a part of three ossicles is in contact with the surface of cochlea. In this research, the cochlea was modeled with the translational springs as shown in Figure 2.14. The cochlea was modeled with a translational in normal direction to the stapes footplate.

2.4 Ligaments

An anterior malleal ligament and a lateral malleal one in four ligaments are muscles supporting the malleus in the middle ear as shown in Figure 2.14. Then, a superior malleal ligament and a posterior incudal one in the other two ligaments are muscles supporting the incus in the middle ear as shown in Figure 2.14. The four ligaments were modeled with the translational springs in this research. Each ligaments was modeled by using six translational springs in normal direction to the ossicles. Three springs were applied for translational motion in x, y and z direction. Then, three springs were applied for rotational motion around x, y, and z axis. The springs constants of each spring were defined by using trial and error method. The ends of four ligaments are connected to the wall of middle ear cavity. Then the ends of four translational springs were clamped.

2.5 Tendons

A posterior stapedial tendon is a muscle located at the head of the stapes as shown in Figure 2.14. The stapes is the smallest bone in a human body. The purposes of posterior

stapedial tendon are to decrease the vibration of the stapes by pulling on the head of the stapes, to prevent excess motion of the stapes, and to control the amplitude of waves in order to protect the inner ear from the loud sounds. In this research, the tendon was modeled with the translational springs. There are six translational springs modeled as a tendon in six degrees of freedom. The translational spring constants were defined by using trial and error method.

2.6. Tensor Tympanic Membrane

A tensor tympanic membrane is a muscle attaching to the malleus as shown in Figure 2.14. The tensor tympanic membrane can regulate the motion of the malleus. If loud sounds are heard, the tensor tympanic membrane reduce the vibration by pulling the malleus away from the eardrum. The tensor tympanic membrane was modelized with the translational spring in this research. The end of the tensor tympanic membrane connects to the wall of middle ear cavity. Then the end of translational spring was clamped.

2.7 Human Ear System

Figure 2.14 shows the shape of middle ear system created using by CAD software. The middle ear consists of an eardrum and three ossicles, namely malleus, incus and stapes. The CAD software, namely Solidworks 2015 was used to create the three dimensional model of the middle ear. The shapes and dimensions of the eardrum were decided by considering the other researchers [3], [22]. Then, the shapes and dimensions of the three ossicles were decided by considering the references [30], [43]. As for the dimensions of malleus, the value of 4.71 [mm] and 8.11 [mm] were used as the length end manubrium to end lateral process and total length of malleus,

respectively. The incus shape has long and short process. The length of long and short process were 6.02 [mm] and 4.58 [mm], respectively. Then as for the stapes dimension, the value of 2.66 [mm], 2.64 [mm] and 1.32 [mm] were used as the height, length of footplate and width of footplate, respectively.

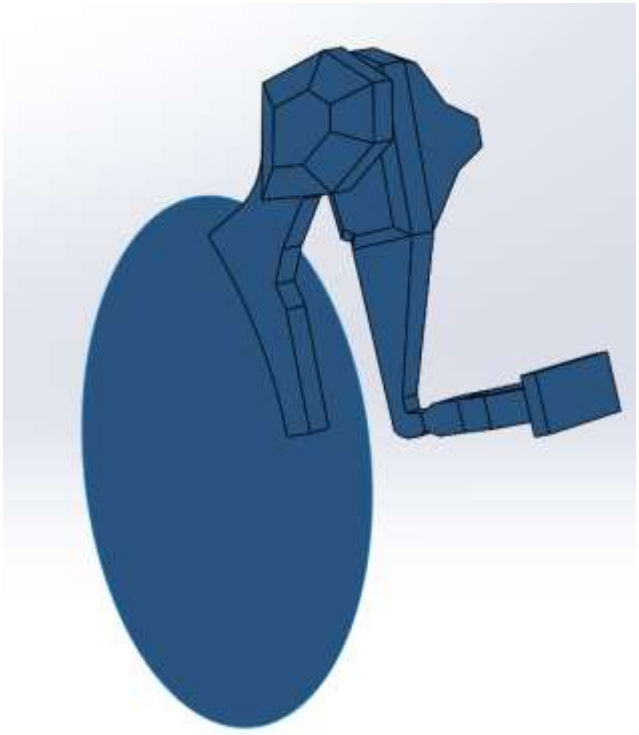

Fig. 2.14 Shape of middle ear system created by using CAD software

A human ear system is composed of the middle ear, the cochlea in inner ear, the four ligaments, the tendon and the tensor tympanic membrane as shown in Figure 2.15. In the finite element model of human ear system, the eardrum and the three ossicles were meshed by using six-node triangular elements and ten-node tetrahedron elements, respectively**.** Then, the material properties of the human middle ear were defined considering the other researchers. [29]

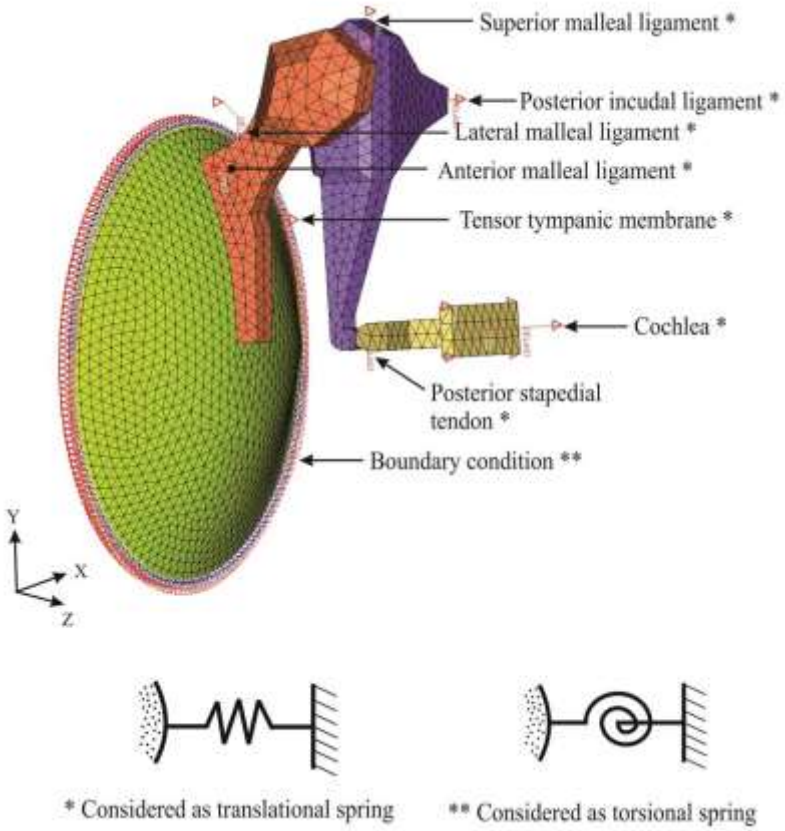

Fig. 2.15 Finite element model of human ear system containing a middle ear, a cochlea in an inner ear, four ligaments, a tendon and a tensor tympanic membrane

2.8 Conclusions

The summary of the results is shown below.

(1) The three-dimensional model of human ear system comprising middle ear system, ligaments, tendon and cochlea had been developed using CAD software (Solidworks 2015) considering the shape and dimension by the other researchers.

(2) In the three dimensional modeling of human eardrum, it was examined that the computational precision in use of the six-node triangular element that is high-order element is better than that of the three-node triangular element that is a low-

order element because the three-node triangular element is the constant strain triangle element.

(3) The new boundary of eardrum modeled with finite elements instead of boundary modeled with torsional springs element had been developed.

Chapter 3

Finite Element Dynamics of Eardrum

3.1 Introduction

The purpose of the study presented in this chapter is to simulate the dynamic behavior of the human eardrum using finite element method. The analysis models of the human eardrum were developed in the chapter 2. Then, the eigenvalue analysis, frequency response analysis was carried out for all analysis model of the human eardrums. Firstly, the eigenvalue and frequency response analyses of the human eardrum with flat shape using clamped boundary condition were carried out. There are two types of elements namely three-node triangular element and six-node triangular element were used for dynamics analysis using finite element method. The comparison between the two types of element are presented in frequency response analysis. Then, dynamics analyses of the eardrum with concave shape were carried out using clamped and torsional springs as boundary conditions. The frequency response of the human eardrum with flat shape and concave shape are presented. Then, the eigenvalue analysis were performed for the eardrum with sliced materials used in myringoplasty. The comparison of vibration modes and natural frequency of the four types of the eardrum

namely normal eardrum, eardrum with a hole, eardrum repaired by sliced cartilage and material are presented. Finally, the dynamics analysis namely eigenvalue and frequency response analysis of the human eardrum were performed.

3.2 Flat Eardrum Using Clamped Boundary Conditions

3.2.1 Material Properties of Eardrum

The material properties of the eardrum the flat eardrum using clamped boundary condition is shown in Table 3.1. The material properties considering the previous published by the other researchers [22].

Table 3.1 Material properties of eardrum

Component	Young's modulus [$\times 10^6$ N/m^2]	Mass density [$\times 10^3$ kg/m^3]	Poisson's ratio [-]*
Eardrum	33	1.2	0.3

*[-] means a dimensionless quantity

3.2.2 Eigenvalue Analysis

In the dynamics analysis of the eardrum, the eigenvalue analysis was carried out to obtain the natural frequencies and the vibration modes of the eardrum without the damping. The natural frequencies and vibration modes can be obtained from the equation of motion by using a homogeneous equation. If there is no damping force, the homogeneous equation becomes

$$\boldsymbol{M}\ddot{\boldsymbol{x}} + \boldsymbol{K}\boldsymbol{x} = \boldsymbol{0} \tag{3.1}$$

In Eq. (3.1), $\boldsymbol{x}$ is assumed by using the fundamental solution, $e^{j\omega t}$ as follows.

$$\boldsymbol{x} = \boldsymbol{x}_o e^{j\boldsymbol{\omega} t} \tag{3.2}$$

where $\boldsymbol{x_o}$ and ω are the amplitude and the angular frequency of the finite element model, respectively. The velocity and acceleration vectors in Eq. (3.1) can be given by the first and second derivatives of the Eq. (3.2) shown as follows.

$$\dot{\boldsymbol{x}} = j\boldsymbol{\omega}\,\boldsymbol{x_o}e^{j\boldsymbol{\omega}t} \tag{3.3}$$

$$\ddot{\boldsymbol{x}} = -\boldsymbol{\omega}^2\boldsymbol{x_o}e^{j\boldsymbol{\omega}t} \tag{3.4}$$

Then, by substituting Eqs. (3.2) and (3.4) into the Eq. (3.1), the following equation can be obtained.

$$-\boldsymbol{\omega}^2\boldsymbol{M}\,\boldsymbol{x_o}\,e^{j\boldsymbol{\omega}t} + \boldsymbol{K}\,\boldsymbol{x_o}\,e^{j\boldsymbol{\omega}t} = \boldsymbol{0} \tag{3.5}$$

After simplifying Eq. (3.5), it becomes

$$\left[-\boldsymbol{\omega}^2\boldsymbol{M} + \boldsymbol{K}\right]\,\boldsymbol{x_o}e^{j\boldsymbol{\omega}t} = \boldsymbol{0} \tag{3.6}$$

In Eq. (3.6), the angular frequency are not equal to zero ($\omega \neq 0$), then Eq. (3.6) should become

$$\left[-\boldsymbol{\omega}^2\boldsymbol{M} + \boldsymbol{K}\right]\,\boldsymbol{x_o} = \boldsymbol{0} \tag{3.9}$$

or

$$\boldsymbol{\omega}^2\boldsymbol{M}\,\boldsymbol{x_o} = \boldsymbol{K}\,\boldsymbol{x_o} \tag{3.10}$$

The Eq. (3.10) can be solved as generalized eigenvalue problem given by

$$\Omega_i^{\,2}\boldsymbol{M}\,\boldsymbol{\phi}_i = \boldsymbol{K}\,\boldsymbol{\phi}_i \tag{3.11}$$

where Ω_i^2, Ω_i and $\boldsymbol{\phi}_i$ denote the i-th eigenvalue, natural angular frequency and eigenvector or vibration mode, respectively.

The i-th natural frequency can be written as follows.

$$f_i = \frac{\Omega_i}{2\pi}\ , \qquad (i = 1, 2, 3\ldots, n) \tag{3.12}$$

3.2.2.1 Calculation Method

The natural frequencies and vibration modes were solved by the eigenvalue analysis. The Optistruct of Hypermesh was used to perform eigenvalue analysis of the flat eardrum. The eigenvalue analysis of the flat eardrum was performed in the frequency range from 100 [Hz] to 10,000 [Hz].

3.2.2.2 Results

There were six natural frequencies less than 1,500 [Hz]. Figure 3.1 shows the first six vibration modes of the flat eardrum. The first vibration mode has one loop in the natural frequency 371 [Hz]. The second vibration mode and the third one have two loops and one node in 733 [Hz] and 810 [Hz] respectively but in different directions. There are two loops and two nodes for the fourth vibration mode and the fifth one in 1,211 [Hz] and 1,284 [Hz], respectively. The sixth vibration mode has one loop and two nodes in 1,482 [Hz].

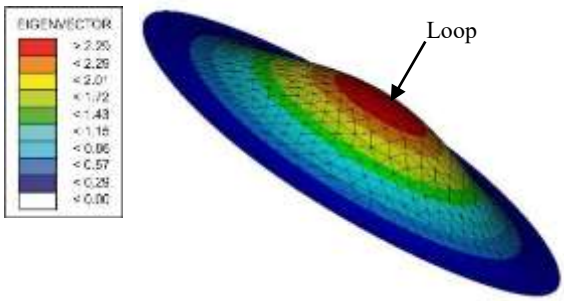

(a) Vibration mode of 1st natural frequency, f_1 = 371 [Hz]

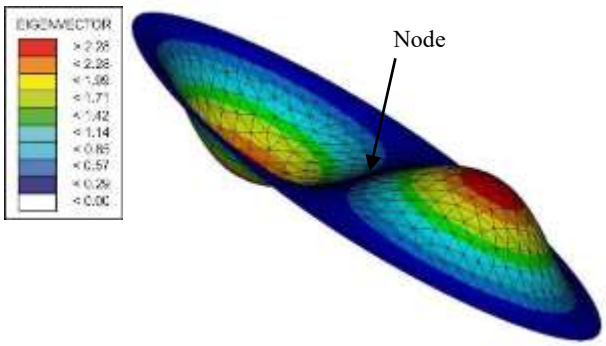

(b) Vibration mode of 2nd natural frequency, f_2 = 733 [Hz]

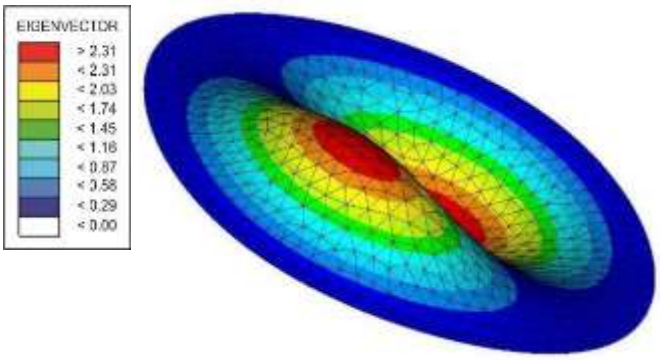

(c) Vibration mode of 3rd natural frequency, f_3 = 810 [Hz]

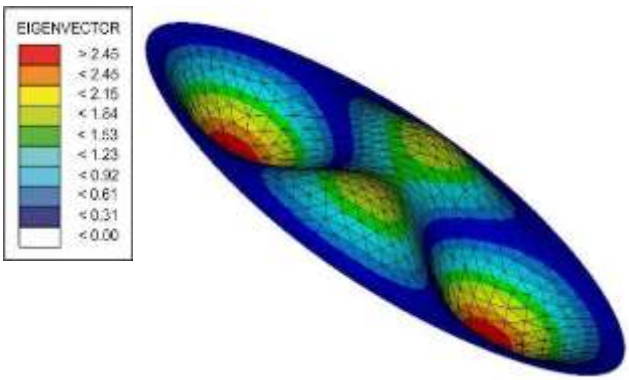

(d) Vibration mode of 4th natural frequency, f_4 = 1,211 [Hz]

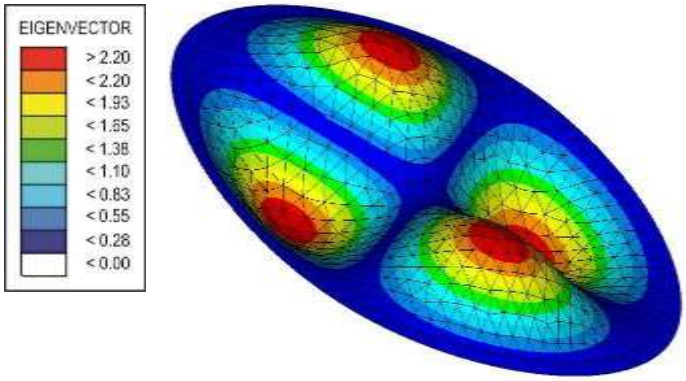

(e) Vibration mode of 5th natural frequency, f_5 = 1,284 [Hz]

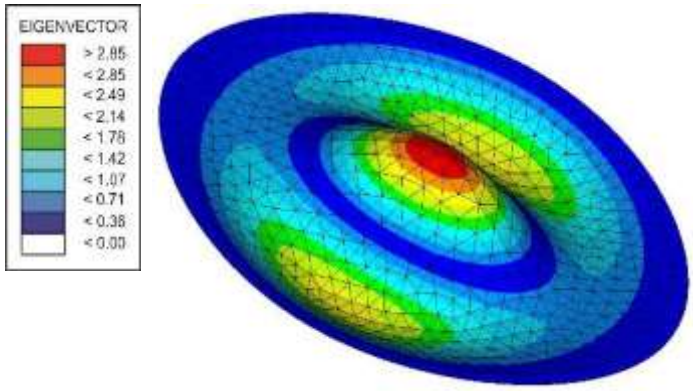

(f) Vibration mode of 6th natural frequency, f_6 = 1,482 [Hz]

Fig. 3.1 Vibration modes of the flat elliptic eardrum using clamped boundary conditions

3.2.3 Frequency Response Analysis

It is well known that there are two methods to perform frequency response analysis namely direct method and modal method. In this research, frequency response analysis of the finite element model was carried out by using modal method. In modal method, the eigenvector or vibration mode of the finite element model was used to uncouple the equation of motions and then the frequency response was obtained by summation of

each modal responses. As for the external force, the harmonic excitation was assumed as follows.

$$\boldsymbol{f} = \boldsymbol{f_o}\, e^{j\omega t} \tag{3.13}$$

Where $\boldsymbol{f_o}$ and ω are the amplitude and the angular frequency of the harmonic excitation. Then, the equation of motion of the finite element model can be written as follows.

$$\boldsymbol{M}\ddot{\boldsymbol{z}} + (1 + jG)\boldsymbol{K}\boldsymbol{z} = \boldsymbol{f}_O e^{j\omega t} \tag{3.14}$$

where $\boldsymbol{z}$ is the displacement. In Eq. (14), the displacement will be transform into the modal displacement. The transformation equation is given by

$$\boldsymbol{z} = \boldsymbol{\phi}\, z(\omega) e^{j\omega t} \tag{3.15}$$

where $z(\omega)$ is the modal displacement. Then, the velocity and the acceleration can be obtained as follows.

$$\dot{\boldsymbol{z}} = j\omega\boldsymbol{\phi}\, z(\omega) e^{j\omega t} \tag{3.16}$$

$$\ddot{\boldsymbol{z}} = -\omega^2\boldsymbol{\phi}\, z(\omega) e^{j\omega t} \tag{3.17}$$

by substituting the Eqs. (3.15) and (3.17) into the Eq. (3.14), the equation of motion becomes

$$-\omega^2\boldsymbol{M}\boldsymbol{\phi}\, z(\omega)\, e^{j\omega t} + (1 + jG)\boldsymbol{K}\boldsymbol{\phi}\, z(\omega) e^{j\omega t} = \boldsymbol{f_o} e^{j\omega t} \tag{3.18}$$

After simplifying the Eq. (3.18), it becomes

$$\left[-\omega^2\boldsymbol{M}\boldsymbol{\phi}\, z(\omega) + (1 + jG)\boldsymbol{K}\boldsymbol{\phi}\, z(\omega) - \boldsymbol{f_o}\right] e^{j\omega t} = 0 \tag{3.19}$$

Multiply the Eq. (19) by $\boldsymbol{\phi}^{\mathrm{T}}$ to uncouple the equation. Then, the following equation can be obtained.

$$-\omega^2\boldsymbol{\phi}^T\boldsymbol{M}\boldsymbol{\phi}\, z(\omega) + (1 + jG)\boldsymbol{\phi}^T\boldsymbol{K}\boldsymbol{\phi}\, z(\omega) = \boldsymbol{\phi}^T\boldsymbol{f_o} \tag{3.20}$$

where $\boldsymbol{\phi}^T \boldsymbol{M}\boldsymbol{\phi}$, $\boldsymbol{\phi}^T \boldsymbol{K}\boldsymbol{\phi}$ and $\boldsymbol{\phi}^T \boldsymbol{f}_o$ are the generalized mass matrix, the generalized stiffness matrix and the modal external force, respectively. The generalized mass matrix and the generalized stiffness matrix are diagonal matrices. As for these diagonal matrices, the equation of motion is uncoupled. In the uncoupled form, the Eq. (3.20) can be written as a set of uncoupled single degree of freedom as follows.

$$-\omega^2 m_i\, z_i(\omega) + (1 + jG_i) k_i\, z_i(\omega) = \boldsymbol{\phi}_i^T \boldsymbol{f_o} \quad (i = 1, 2, 3, \ldots, n) \tag{3.21}$$

where m_i and k_i are i-th modal mass and i-th modal stiffness, respectively. Each of the modal responses can be obtained using

$$z_i(\omega) = \frac{\boldsymbol{\phi}_i^T \boldsymbol{f_o}}{(1 + jG_i) k_i - \omega^2 m_i} \tag{3.22}$$

or

$$z_i(\omega) = \frac{\boldsymbol{\phi}_i^T \boldsymbol{f_o} \big/ m_i}{\Omega_i^2 + jG_i\, \Omega_i^2 - \omega^2} \tag{3.23}$$

The displacement can be obtained by summation of the modal responses shown as follows

$$\boldsymbol{z} = \sum_{i=1}^{n} \boldsymbol{\phi}_i\, z_i(\omega) e^{j\omega t} \tag{3.24}$$

3.2.3.1 Calculation Method

The Optistruct (Solver) of HyperMesh was used to carry out the frequency response analysis. The three-node and six-node triangular elements were used in this analysis. The frequency response analysis of flat eardrum was performed under the sound pressure level, $P = 2.0 \times 10^{-5}$ [Pa] in the frequency range 100 [Hz] to 10,000 [Hz]. As

for the pressure load of frequency response analysis, the direction of pressure load was normal to the element as shown in the Fig. 3.2.

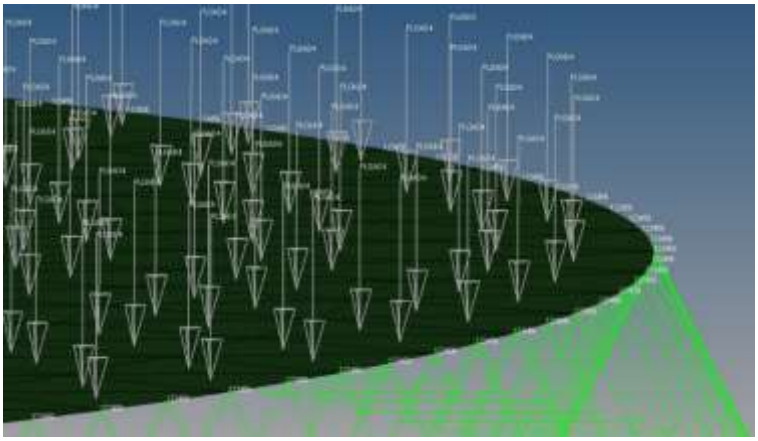

Fig. 3.2 Sound pressure level normal to the flat eardrum.

3.2.3.2 Result

The frequency responses on umbo displacement of the flat eardrum under sound pressure level, $P = 2 \times 10^{-5}$ [Pa] are shown in Fig. 3.3. The three-node and six-node triangular elements were used. It can be seen that the result using the six-node triangular elements was different from the one using the three-node ones. The three-node triangular element is constant strain triangular element. In which the strain is constant inside the element. Then it is well known that the computational precision is not good for the three-node triangular element. For this reason, the six-node triangular elements were used in this research.

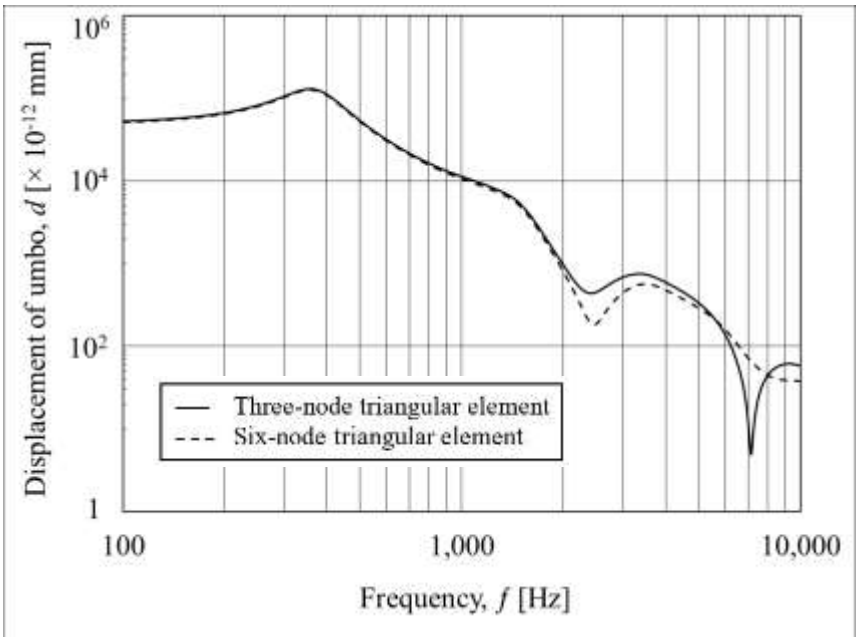

Fig. 3.3 Frequency responses on umbo displacement of the flat eardrum under sound pressure level, $P = 2 \times 10^{-5}$ [Pa]

3.3 Concave Eardrum Using Clamped Boundary Condition

3.3.1 Eigenvalue Analysis

3.3.1.1 Calculation Method

The eigenvalue analysis of the concave eardrum using clamped boundary condition was carried out in the same frequency range with the flat eardrum. The eigenvalue analysis was used to obtain the natural frequencies and the vibration modes of the concave eardrum using clamped boundary condition.

3.3.1.2 Results

Figure 3.4 shows the vibration mode of the concave eardrum using clamped boundary conditions less than 1,500 [Hz]. In that frequency range, six natural

frequencies were solved. The first vibration mode of the concave eardrum has two loops and two nodes in 2,919 [Hz]. Then, the second vibration mode has one loop in the major axis direction and two nodes in 3,030 [Hz]. For the third vibration mode and the fourth one have similar modes. There are three loops and three nodes for the third vibration mode and the fourth one in 3,061 [Hz] and 3,064 [Hz], respectively. The fifth vibration mode and the sixth one have more complex modes. The fifth vibration mode has three loops and three nodes in 3,378 [Hz]. Finally, the sixth vibration mode has four loops and four nodes in 3,422 [Hz].

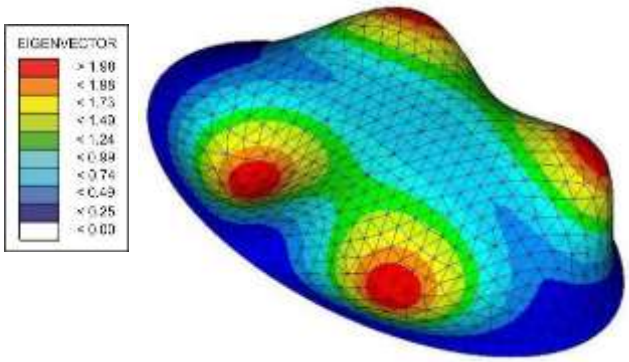

(a) Vibration mode of 1st natural frequency, f_1 = 2,919 [Hz]

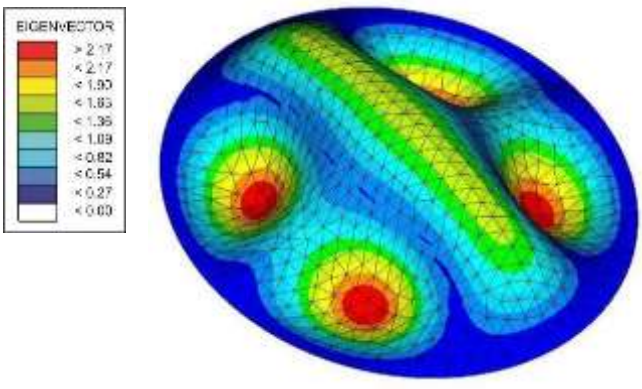

(b) Vibration mode of 2nd natural frequency, f_2 = 3,030 [Hz]

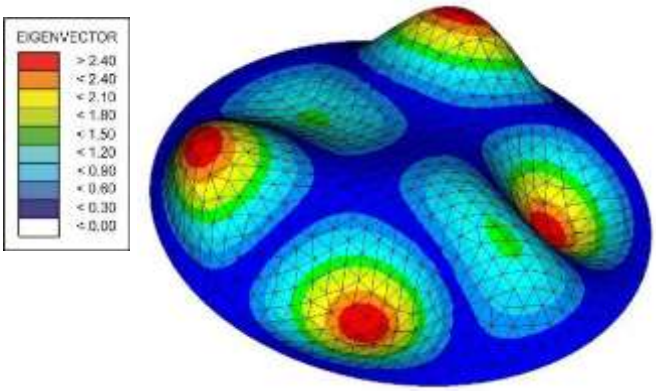

(c) Vibration mode of 3rd natural frequency, f_3 = 3,061 [Hz]

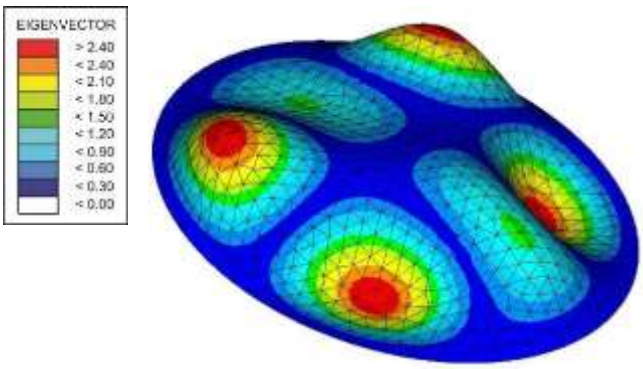

(d) Vibration mode of 4th natural frequency, f_4 = 3,064 [Hz]

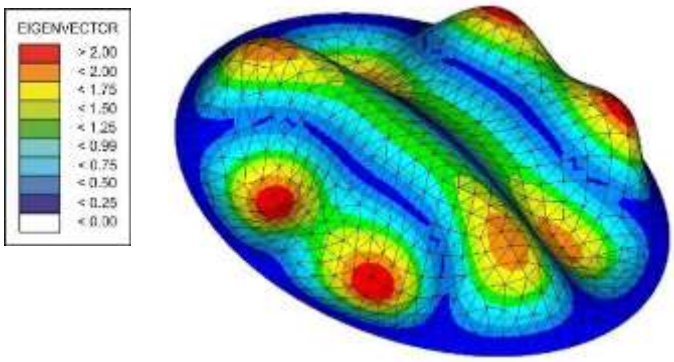

(e) Vibration mode of 5th natural frequency, f_5 = 3,378 [Hz]

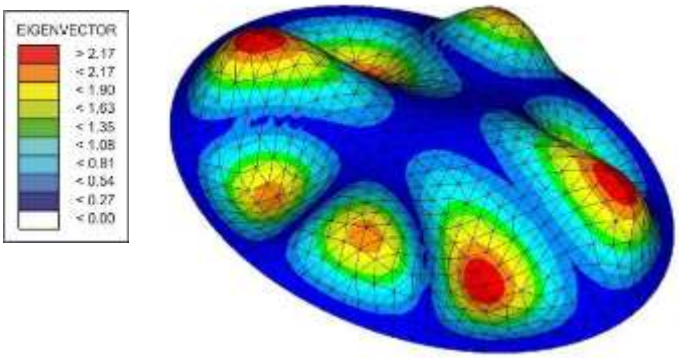

(f) Vibration mode of 6th natural frequency, f_6 = 3,422 [Hz]

Fig. 3.4 Vibration modes of the concave eardrum using clamped boundary conditions

3.3.2 Frequency Response Analysis

3.3.2.1 Calculation Method

Under the same sound pressure and the same frequency range as the flat eardrum, the frequency response analysis of the concave eardrum using clamped boundary condition was performed using the Optistruct of HyperMesh. Then, the value of G = 0.4 was used as structural damping of concave eardrum using clamped boundary condition.

3.3.2.2 Result

Figure 3.5 shows the frequency responses of umbo displacement for the flat eardrum and the concave eardrum with clamped boundary conditions under sound pressure level, $P = 2 \times 10^{-5}$ [Pa]. This results shows that the first natural frequency of the flat eardrum is lower than the one of the concave eardrum. It is desired that the responses become constant in frequency response characteristics of an eardrum. Human being can hear

sounds well if they have an eardrum having the above characteristics. Then we can understand that a concave eardrum is better than a flat one like the flat eardrum.

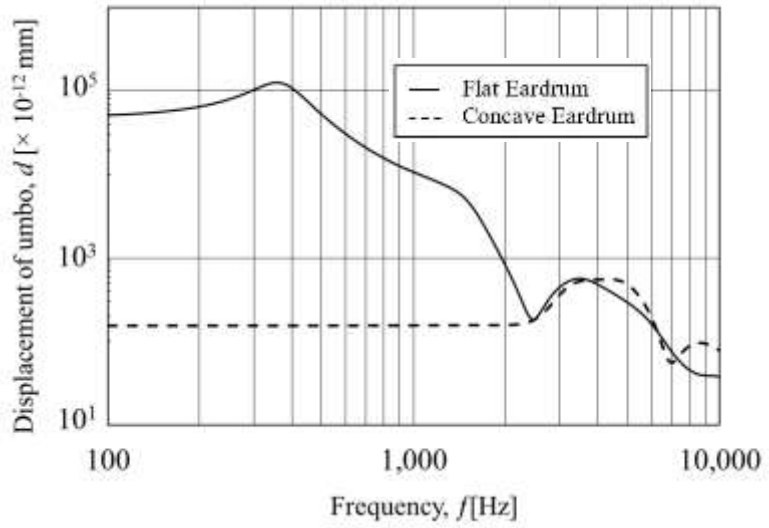

Fig. 3.5 Frequency responses of umbo displacement for the flat eardrum and the concave eardrum with clamped boundary conditions under sound pressure level, $P = 2 \times 10^{-5}$ [Pa]

3.4 Concave Eardrum Using Torsional Springs as Boundary Conditions

3.4.1 Eigenvalue Analysis

3.4.1.1 Calculation Method

The eigenvalue analysis of the concave eardrum using torsional springs as boundary conditions was carried out to obtain the natural frequencies and the vibration modes in the frequency range from 100 [Hz] to 10,000 [Hz]. The torsional spring constant, $K_\theta = 3.0 \times 10^{-5}$ [Nmm/rad] was used for the rotational motion around the y-axis on the boundary of the eardrum considering by the other researcher. The torsional springs were used as boundary condition in order to the boundary of the eardrum same as the real human eardrum.

3.4.1.2 Results

Figure 3.6 shows the vibration modes of concave eardrum using the torsional spring constant, $K\theta$ = 3.0 × 10^{-5} [Nmm/rad] on the boundary. The first, second and third vibration modes have similar modes. Their vibration modes have two large loops and two small ones in f_1 = 2,599 [Hz], f_2 = 2,616 [Hz] and f_3 = 2,621 [Hz], respectively. The fourth vibration mode has one large loop and two small ones in f_4 = 2,661 [Hz]. The fifth vibration mode has four loops in f_5 = 3,012 [Hz]. Then, the sixth vibration mode has eight loops in f_6 = 3,116 [Hz].

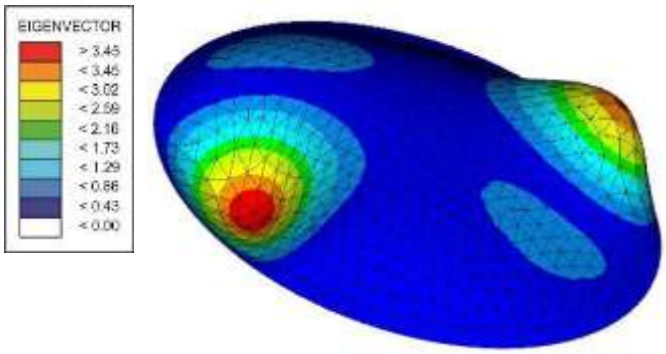

(a) Vibration mode 1st natural frequency, f_1 = 2,599 [Hz]

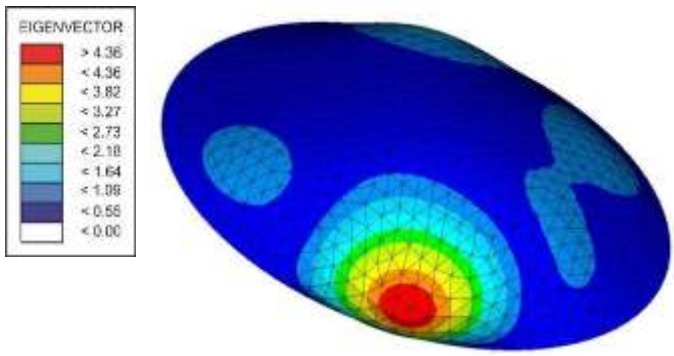

(b) Vibration mode 2nd natural frequency, f_2 = 2,616 [Hz]

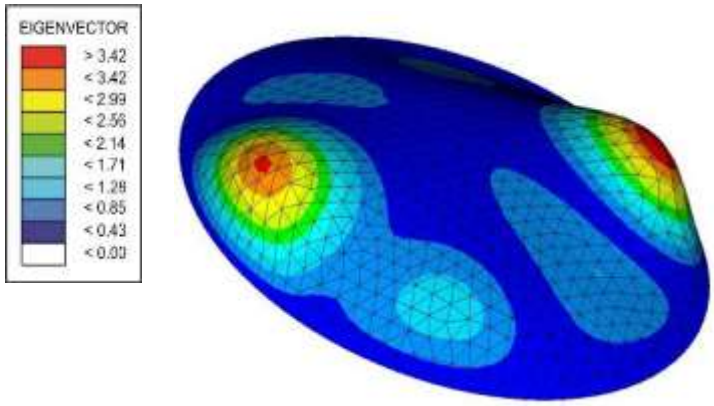

(c) Vibration mode 3rd natural frequency, f_3 = 2,621 [Hz]

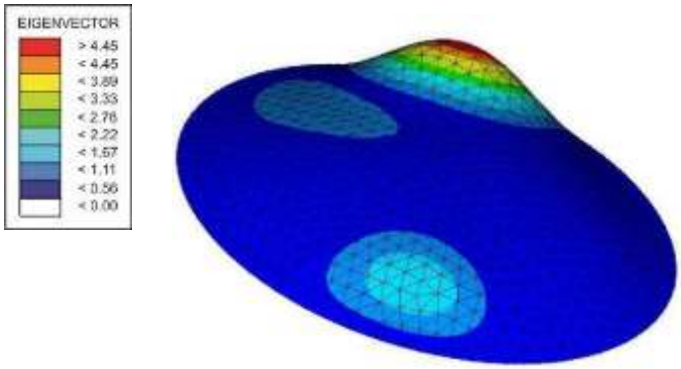

(d) Vibration mode 4th natural frequency, f_4 = 2,661 [Hz]

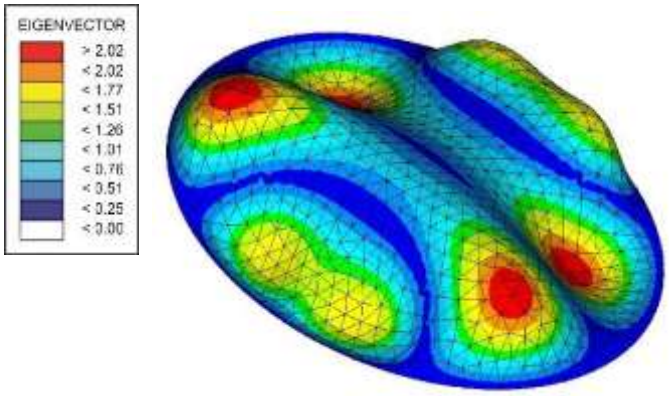

(e) Vibration mode 5th natural frequency, f_5 = 3,012 [Hz]

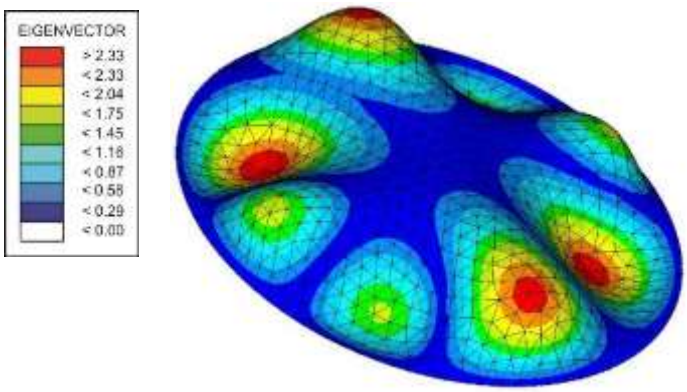

(f) Vibration mode 6th natural frequency, f_6 = 3,116 [Hz]

Fig. 3.6 Vibration modes of concave eardrum using the torsional spring constant, K = 3.0×10^{-5} [Nmm/rad] on the boundary of the eardrum

3.4.2 Frequency Response Analysis

3.4.2.1 Calculation Method

The Optistruct of HyperMesh was used as the solver to perform the frequency response analyses of flat eardrum using clamped boundary conditions and concave eardrum using the torsional springs on the boundary under the sound pressure level, $P = 2.0 \times 10^{-5}$ [Pa] in the frequency range from 100 [Hz] to 10,000 [Hz]. As for the structural damping coefficient, G, the value of $G = 0.4$ proposed by the other researchers [1] was used. Two kinds of values on the torsional spring constants were used on the boundary of the concave eardrum. The torsional spring constant, $K_\theta = 0.1$ [Nmm/rad] was used so that the result can be similar to that with the clamped boundary conditions. Then the torsional spring constants, $K_\theta = 3.0 \times 10^{-5}$ [Nmm/rad] proposed by the other researchers [22] was used so that the results can be similar to those of a human ear.

3.4.2.2 Result

Figure 3.7 shows the frequency responses on displacement of umbo of flat eardrum using clamped boundary conditions and concave eardrum using torsional spring on the boundary under the sound pressure level, $P = 2.0 \times 10^{-5}$ [Pa]. The results show that the fist natural frequency of flat eardrum is quite lower than them of concave eardrum. A frequency response of a human ear is desired to be constant in a broad frequency range. A human being can easily hear sounds well if the frequency response of an eardrum has the above characteristics. Then, it means that a concave shape is better than a flat one like flat eardrum as a shape of an eardrum. It is assumed that a shape of a human eardrum may be a concave one in the process of evolution.

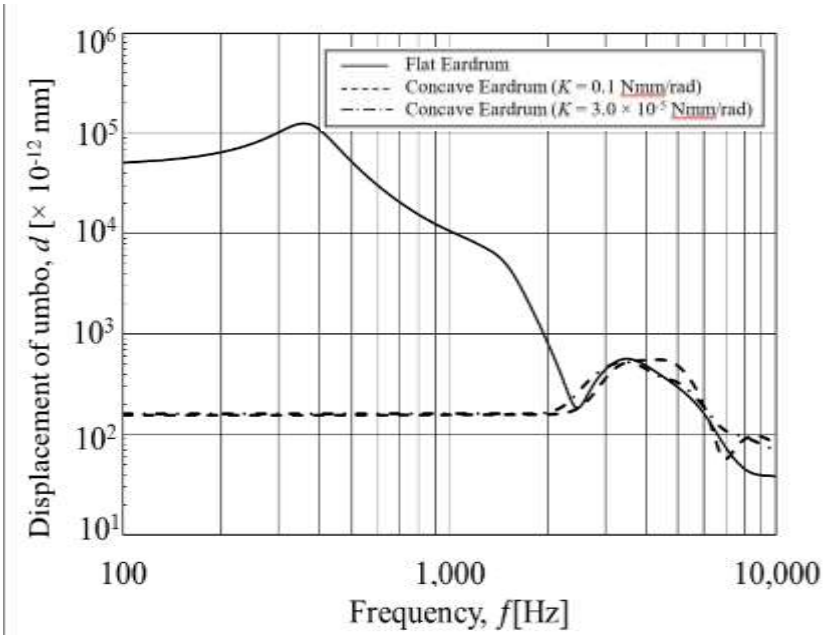

Fig. 3.7 Frequency responses on displacement of umbo of flat eardrum using clamped boundary conditions and concave eardrum using torsional spring on the boundary under the sound pressure level, $P = 2.0 \times 10^{-5}$ [Pa]

3.5 Eardrum with Sliced Materials used in Myringoplasty

3.4.1 Eigenvalue Analysis

3.4.1.1 Calculation Method

The Optistruct of Hypermesh was used to carry out eigenvalue analysis of the four types of the eardrums. The eigenvalue analysis was carried out to obtain natural frequencies and vibration mode of the four types of the eardrums in the frequency range from 100 [Hz] to 10,000 [Hz]. The proper thickness of both sliced cartilage and sliced material having the same material properties as the human eardrum were examined in order to obtain the similar vibration modes as the normal eardrum.

In order to obtained the proper thickness of both sliced cartilage and sliced material having the same material properties as the human eardrum using eigen-value analysis, the comparison of vibration modes and natural frequencies between sliced cartilage and sliced material were carried out. Figure 3.8 shows the sliced cartilage and sliced material used in myringoplasty of humans. In this analysis model, two layers of element, namely eardrum and sliced cartilage or material were developed. The shape of eardrum like ring have outside and inside diameter, D = 2.7 [mm] and D = 2.5 [mm], respectively. Then, the sliced cartilage and material have diameter, D = 2.7 [mm].

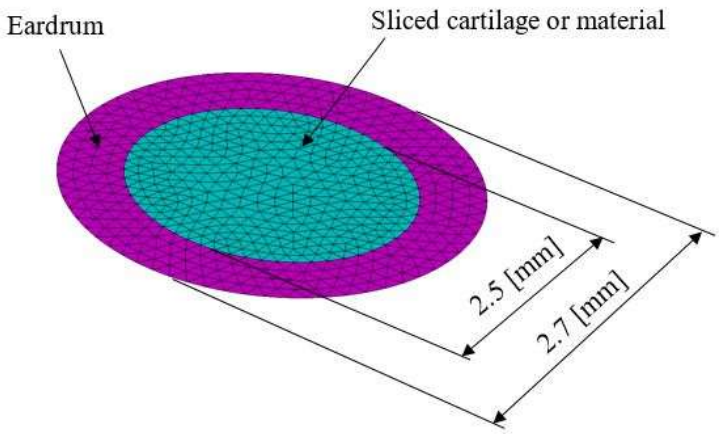

Fig 3.8 Sliced cartilage and sliced material used in myringoplasty of humans

The angular natural frequencies of sliced cartilage and sliced material can be expressed using the equation as shown below.

$$\omega_{c,m} = \alpha_{dc} \frac{t_{c,m}}{R^3} \sqrt{\frac{E_{c,m}\, g}{(1-\upsilon^2)\, \gamma_{c,m}}} \tag{3.1}$$

where α_{dc}, $t_{c,m}$, R and g are the dimensionless coefficient, thickness, radius of sliced cartilage or material and gravitational acceleration, respectively. Then, E, υ and γ denote the Young's modulus, Poisson's ratio and mass density, respectively.

In this case, the radius, gravitational acceleration and Poisson's ratio of the sliced cartilage are the same as sliced material. Then, in order to obtain the same natural frequencies between sliced cartilage and sliced material having the same material properties as the human eardrum, the Eq. (3.1) become

$$t_c \sqrt{\frac{E_c}{\gamma_c}} = t_m \sqrt{\frac{E_m}{\gamma_m}} \tag{3.2}$$

After simplifying Eq. (3.2), it becomes

$$t_c = t_m \sqrt{\frac{E_m \gamma_c}{E_c \gamma_m}} \tag{3.3}$$

The thickness of sliced material having the same material properties as the human eardrum can be assumed as t = 0.1 [mm]. Then, the value of t_c = 0.358 [mm] was obtained as the thickness of sliced cartilage using Eq. (3.3). Furthermore, the thickness of sliced cartilage t = 0.4 [mm] was used to carry out eigen-value analysis of the eardrum repaired by sliced cartilage.

3.4.1.2 Results

Figure 3.9 shows the vibration modes of the four types of eardrums. As for the vibration modes of the eardrum with a hole, the main mode shapes appeared around the hole. Usage of the sliced material with thickness, t = 0.1 [mm] having the same material properties as the normal eardrum was recommended so that its vibration modes can become the similar ones as the normal eardrum.

As for the eardrum repaired by sliced cartilage used in myringoplasty, when the value of t = 0.4 [mm] was used as the thickness of sliced material, the vibration modes of the 1st and 2nd natural frequencies became of the similar ones as those of the normal eardrum.

Then, the vibration modes of the 3rd, 4th, 5th and 6th natural frequencies became the similar ones as the normal eardrum when the value of t = 0.45[mm] was used as the thickness of sliced cartilage.

ormal eardrum with thickness, t = 0.1 [mm]	Eardrum with thickness, t = 0.1 [mm] having the hole with diameter, D = 2.5 [mm]	Eardrum with thickness, t = 0.1 [mm] repaired by the sliced material with thickness, t = 0.1 [mm] having the same material properties as the eardrum	Eardrum with thickness, t = 0.1 [mm] repaired by the sliced cartilage having the similar vibration mode as the normal eardrum
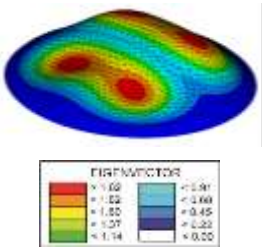 Vibration mode of 1st natural frequency, f_1 = 3,062 [Hz]	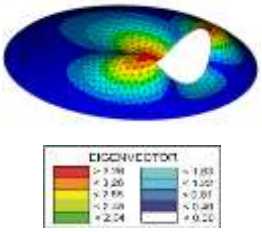 Vibration mode of 1st natural frequency, f_1 = 2,240 [Hz]	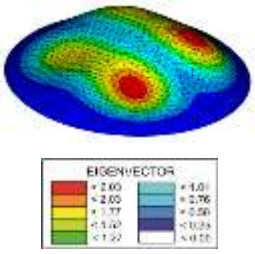 Vibration mode of 1st natural frequency, f_1 = 3,040 [Hz]	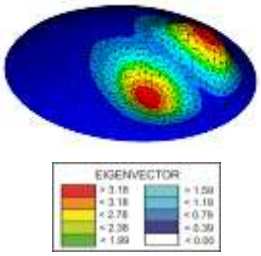 Vibration mode of 2nd natural frequency, f_2 = 2,146 [Hz] using cartilage thickness, t = 0.4 [mm]
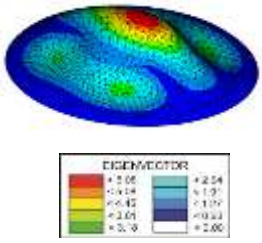 Vibration mode of 2nd natural frequency, f_2 = 3,183 [Hz]	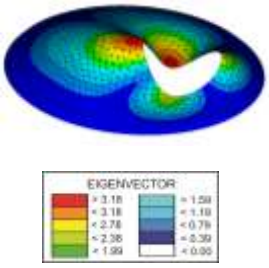 Vibration mode of 2nd natural frequency, f_2 = 2,334 [Hz]	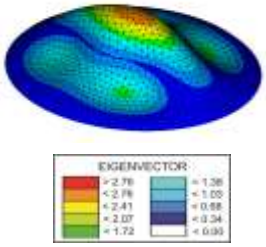 Vibration mode of 2nd natural frequency, f_2 = 3,161 [Hz]	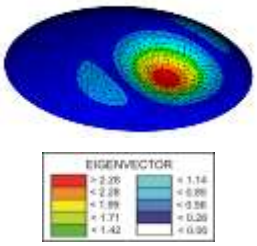 Vibration mode of 1st natural frequency, f_1 = 1,751 [Hz] using cartilage thickness, t = 0.4 [mm]
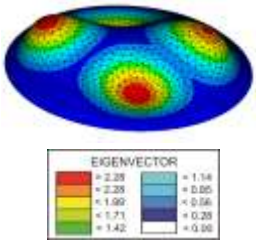 Vibration mode of 3rd natural frequency, f_3 = 3,308 [Hz]	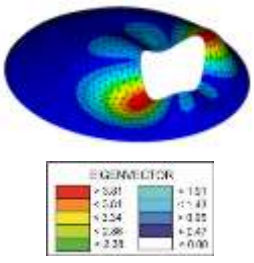 Vibration mode of 3rd natural frequency, f_3 = 3,065 [Hz]	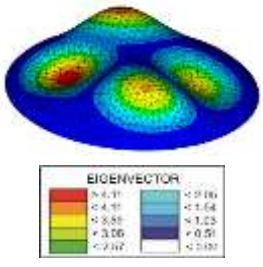 Vibration mode of 3rd natural frequency, f_3 = 3,276 [Hz]	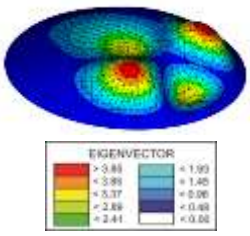 Vibration mode of 4th natural frequency, f_4 = 2,832 [Hz] using cartilage thickness, t = 0.45 [mm]

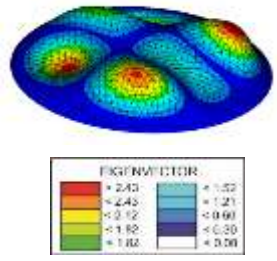	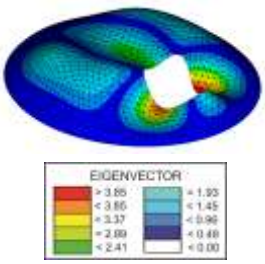	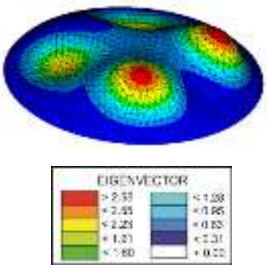	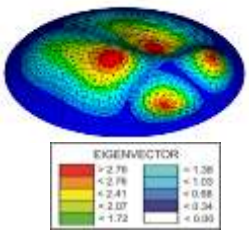
Vibration mode of 4th natural frequency, f_4 = 3,440 [Hz]	Vibration mode of 4th natural frequency, f_4 = 3,182 [Hz]	Vibration mode of 4th natural frequency, f_4 = 3,425 [Hz]	Vibration mode of 5th natural frequency, f_5 = 2,834 [Hz] using cartilage thickness, t = 0.45 [mm]
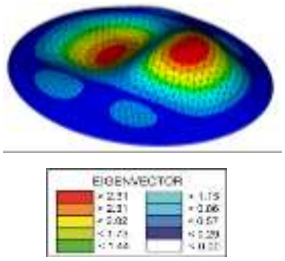	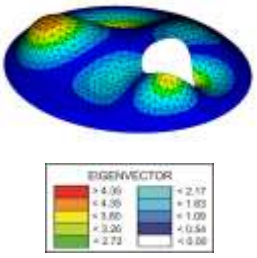	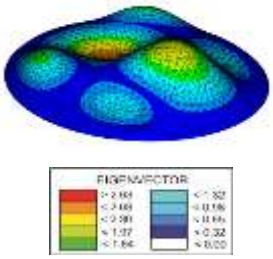	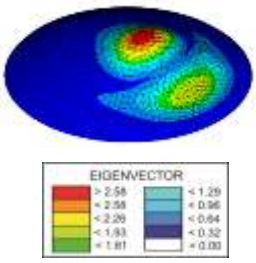
Vibration mode of 5th natural frequency, f_5 = 3,532 [Hz]	Vibration mode of 5th natural frequency, f_5 = 3,290 [Hz]	Vibration mode of 5th natural frequency, f_5 = 3,443 [Hz]	Vibration mode of 5th natural frequency, f_5 = 2,834 [Hz] using cartilage thickness, t = 0.45 [mm]
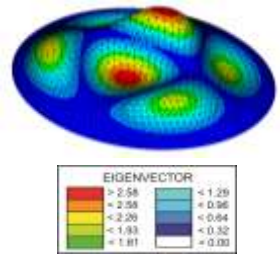	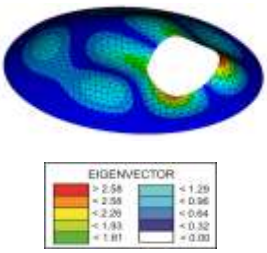	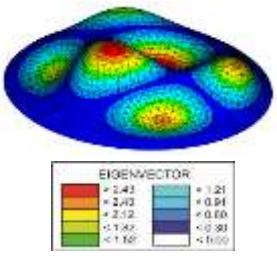	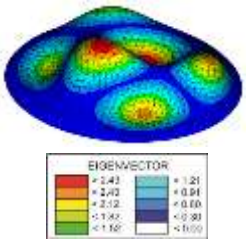
Vibration mode of 6th natural frequency, f_6 = 3,552 [Hz]	Vibration mode of 6th natural frequency, f_6 = 3,407 [Hz]	Vibration mode of 6th natural frequency, f_6 = 3,535 [Hz	Vibration mode of 5th natural frequency, f_6 = 3,234 [Hz] using cartilage thickness, t = 0.45 [mm]

Fig. 3.9 Vibration modes of the four types of eardrums

Figure 3.10 shows the effect of sliced material having the same material properties as the eardrum and the sliced cartilage on natural frequencies. The natural frequencies of the eardrum repaired by sliced material having the same material properties as the normal eardrum approached those of the normal eardrum when the value of t = 0.1 [mm] was used as the thickness of the sliced material. The natural frequencies of the eardrum repaired by the sliced cartilage became lower than those of the normal eardrum or the eardrum repaired by the sliced material having the same material properties as the normal eardrum. The reason why the natural frequencies of the former were lower than those of the latter is thought as follows.

The thickness of the sliced cartilage should be made to t = 0.4 [mm] in order to match vibrational characteristics of the sliced cartilage with those of the sliced material having the same material properties as an eardrum. In this case, the mass of the sliced cartilage becomes four times as that of the other. It is thought that the effect of this large mass of a sliced cartilage may decrease the natural frequencies of the eardrum repaired by the sliced cartilage than those of the other. Then, the natural frequencies of the eardrum repaired by sliced cartilage approached the 1st natural frequency of the normal eardrum when the thickness of t = 0.35 [mm] was used. While, when considering the vibration modes shown in Fig. 3.9, using the thickness of t = 0.4 [mm] as that of the sliced cartilage could give the most similar vibration modes as those of the normal eardrum. Furthermore, the 2nd, 3rd, 4th, 5th, and 6th natural frequencies of the eardrum repaired by sliced cartilage with thicknesses from t = 0.15 [mm] to 0.5 [mm] approached those of the normal eardrum in Fig. 3.10. Consequently, it is thought that the proper thicknesses of sliced cartilage used in myringoplasty are from 0.4 [mm] to 0.45 [mm] by considering the calculated results in a comprehensive way.

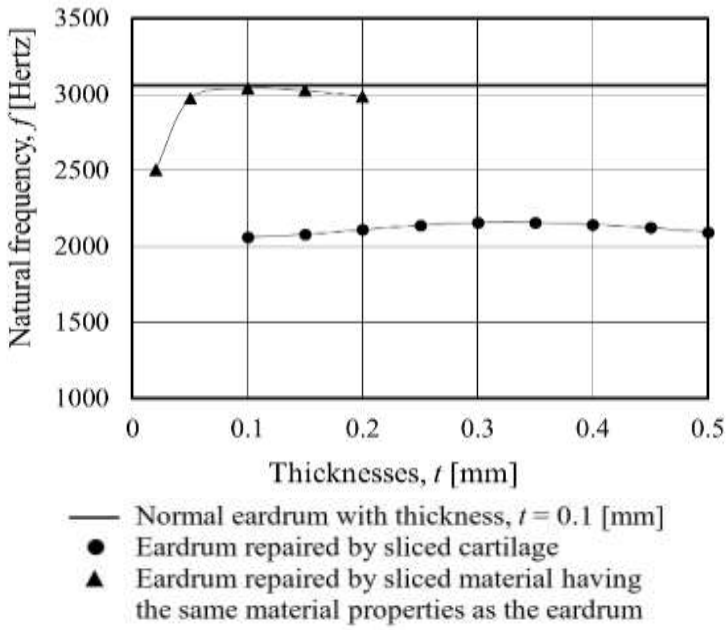

(1) Natural frequencies of the eardrum repaired by the sliced material having the same material properties as the eardrum and the eardrum repaired by the sliced cartilage that have the similar mode shape as 1st natural frequency of the normal eardrum

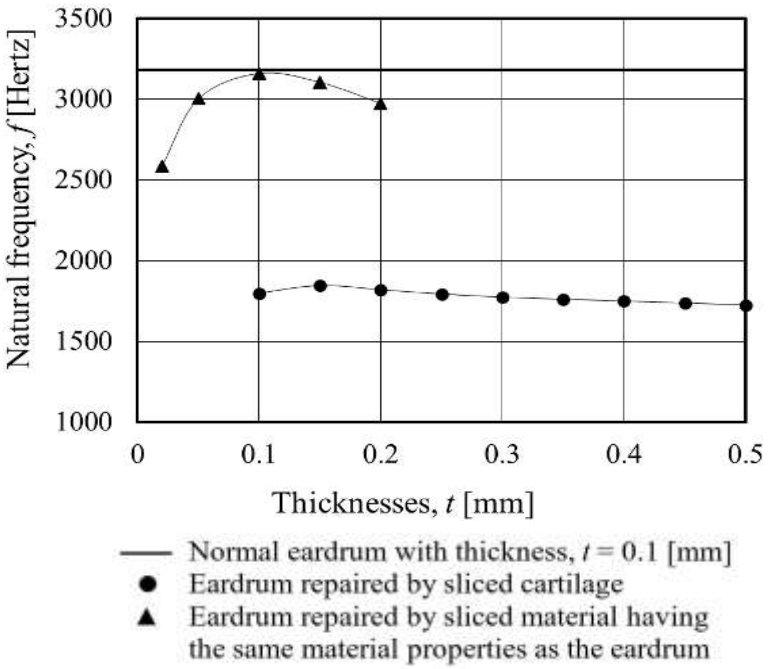

(2) Natural frequencies of the eardrum repaired by the sliced material having the same material properties as the eardrum and the eardrum repaired by the sliced cartilage that have the similar mode shape as 2nd natural frequency of the normal eardrum

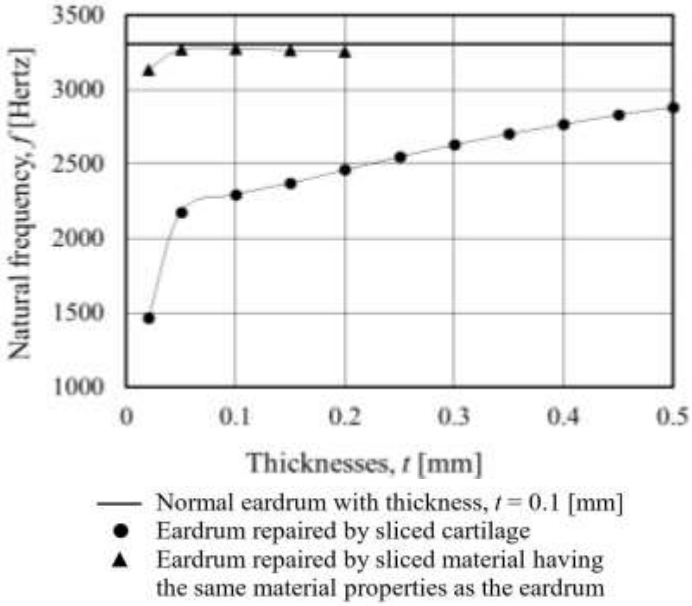

(3) Natural frequencies of the eardrum repaired by the sliced material having the same material properties as the eardrum and the eardrum repaired by the sliced cartilage that have the similar mode shape as 3rd natural frequency of the normal eardrum

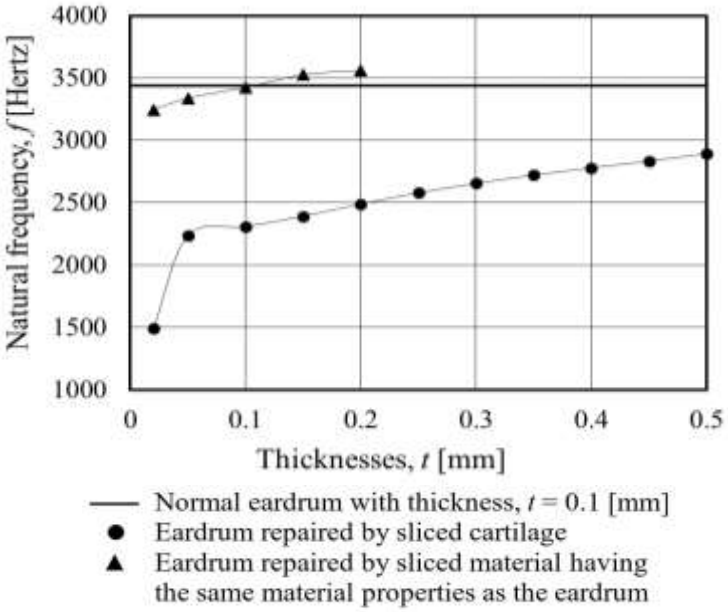

(4) Natural frequencies of the eardrum repaired by the sliced material having the same material properties as the eardrum and the eardrum repaired by the sliced cartilage that have the similar mode shape as 4th natural frequency of the normal eardrum

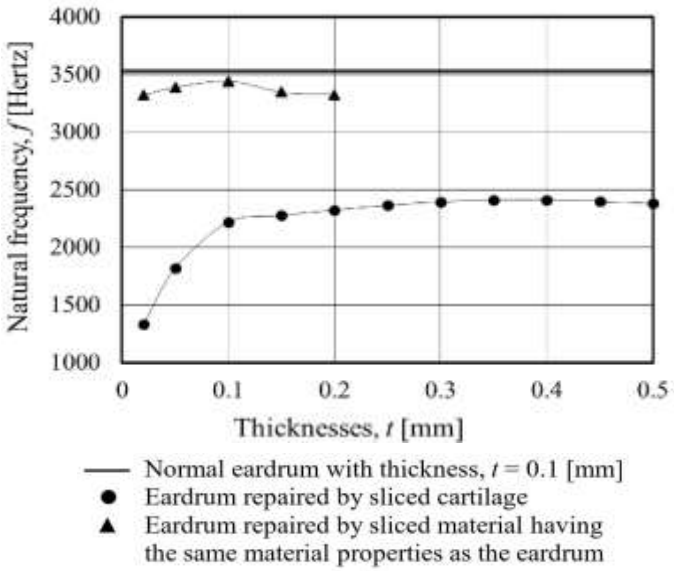

(5) Natural frequencies of the eardrum repaired by the sliced material having the same material properties as the eardrum and the eardrum repaired by the sliced cartilage that have the similar mode shape as 5th natural frequency of the normal eardrum

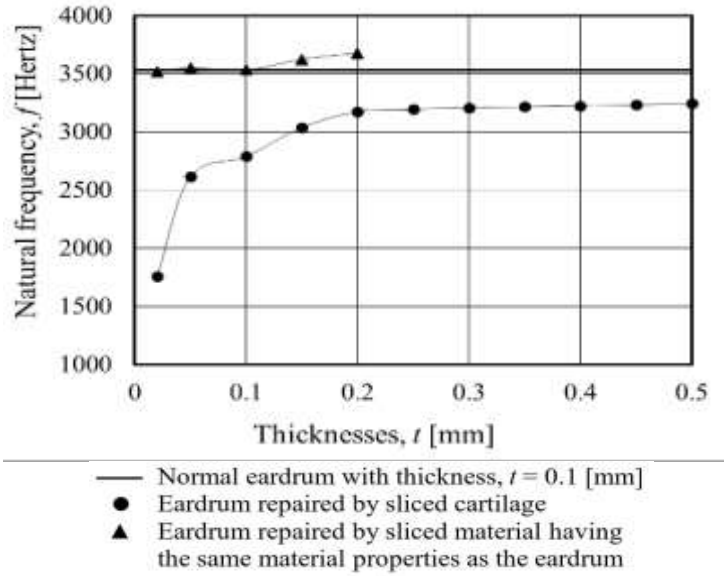

(6) Natural frequencies of the eardrum repaired by the sliced material having the same material properties as the eardrum and the eardrum repaired by the sliced cartilage that have the similar mode shape as 6th natural frequency of the normal eardrum

Fig. 3.10 Effect of sliced material having the same material properties as the eardrum and the sliced cartilage on natural frequencies

3.6 Conclusions

The summary of results is shown below

1. The eigen-value and frequency response analysis of flat eardrum using clamped boundary condition, concave eardrum using two types boundary condition, namely clamped and torsional springs had been carried out.
2. The new boundary of eardrum modeled finite elements having the same dynamic behavior as the boundary modeled with torsional springs that is similar to those of human eardrum had been carried out.
3. It was determined that the proper thicknesses of the sliced cartilage were 0.45 [mm] to 0.45 [mm] and sliced material having the same material properties as the human eardrum was 0.1 [mm] using the eigen-value analysis by comparing the vibration modes and natural frequencies of the four types of the eardrums.

Chapter 4

Finite Element Dynamics of Human Ear System

4.1 Introduction

The purpose of the study presented in this chapter is to simulate dynamic behavior of human ear system using finite element method. The human ear system in this chapter is composed of middle ear, cochlea in inner ear, ligaments, tendon and tensor tympanic membrane. Eigenvalue, frequency response and time history response analysis were performed for human ear system using torsional spring as boundary condition and boundary modeled with finite elements. Then five structural damping coefficients were used for the frequency response analyses to examine the effect of structural damping coefficients on the displacements of stapes in 1,500 [Hz] and more. In the time history response analysis of human ear system using torsional springs as boundary conditions, format frequencies and human voices were used as external forces. The human voices downloading from a website opening sample as wav files were used. As for the human ear systems using boundary modeled with finite elements, four types of eardrum were used for each human ear system. Then, frequency response analyses were performed to compare the response of the four types of human ear system. Finally, the time history

response analyses of the four types of human ear system were carried out using human voices as input sound pressures in order to confirm the effects of the sliced materials in myringoplasty.

4.2 Material Properties of Middle Ear

Table 1 shows the material properties of middle ear used in the present calculations. The values in Table 1 were decided by considering the references [22], [43].

Table 1. Material properties of middle ear.

Structure	Young's modulus [$\times 10^9$ N/m^2]	Mass density [$\times 10^{-9}$ kg/m^3]	Poisson's ratio [-]*
Eardrum	0.033	1.20	0.3
Malleus	14.0	2.55	0.3
Incus	14.0	2.36	0.3
Stapes	14.0	2.20	0.3

* [-] means a dimensionless quantity

4.3 Spring Constants and Boundary Conditions

Table 2 shows the translational spring constants of ligaments, a tendon, a tensor tympanic membrane and a cochlea. As for the ligaments, the tendon and the tensor tympanic membrane, each of them was considered as three translational springs in *x, y* and *z* directions. The indexes, *x*, *y* and *z* of each spring constant denote the local coordinates of itself. The *x*-direction of each local coordinate frame was defined in the normal direction to the surface of an ossicle. The values of translational spring constants, K_i ($i = x, y, z$) for the ligaments, the tendon, the tensor tympanic membrane and the cochlea were decided by trial and error so that the stapes can perform a piston motion in

the *x*-direction of local coordinate frame. The stapes contacting with the cochlea moves like a piston in the *x*-direction.

Table 2. Translational spring constants of ligaments, a tendon, a tensor tympanic membrane and a cochlea.

Component	Spring constant, K_x [N/mm]	Spring constant, $K_y = K_z$ [N/mm]
Anterior malleal ligament	1.2	0.3
Lateral malleal ligament	1.2	0.3
Superior malleal ligament	1.2	0.3
Posterior incudal ligament	1.2	0.3
Tensor tympanic membrane	1.2	0.3
Posterior stapedial tendon	1.2	0.3
Cochlea	0.2	-

As for the boundary conditions of the eardrum, a local coordinate frame was defined at each node of boundary of the eardrum. In each the local coordinate frame, three translational motions in the *x*-, *y*- and *z*- directions and two rotational ones around the *x*-, and *z*- axes were clamped. Then, the torsional springs of $K_{\theta y}$ were applied to the rotational motions around the y-axes, on the nodes of boundary of the eardrum. The torsional springs of $K_{\theta y}$ were used to adjust the stiffness of boundary of the eardrum in order to make the boundary conditions of the eardrum similar to those of a human eardrum. As for the torsional springs on boundary of the eardrum, the same values, $K_{\theta y} = 3.0\times10^{-5}$ [Nmm/rad] as the authors' previous report were used [22].

4.4 Human Ear System Using Torsional Springs as Boundary Conditions

4.4.1 Eigenvalue Analysis

4.4.1.1 Calculation Method

The Optistruct of Hypermesh was used to carry out eigen-value analysis of human ear system using torsional springs as boundary conditions. The eigen-value analysis of the human ear system was carried out to obtain the natural frequencies and the vibration modes in the frequency range from 100 [Hz] to 10,000 [Hz].

4.4.1.2 Results

Figure 4.1 shows the vibration modes of the human ear system. The first, second and third vibration modes have similar modes, but the directions of motions of the three ossicles are different. Then the first vibration mode has one small loop. The three ossicles move in the normal direction to the surface of the eardrum in f_1 = 1,033 [Hz]. The second vibration mode in f_2 = 1,728 [Hz] has two small loops. The directions of motions of the three ossciles in f_2 = 1,728 [Hz] are different from the first one in f_1 = 1,033 [Hz]. Furthermore, the third vibration mode in f_3 = 1,846 [Hz] has two small loops, and the directions of motions of the three ossicles are different. The fourth, fifth and sixth vibration modes have similar modes in which the displacements at loops of the three ossicles are very small. The fourth vibration mode in f_4 = 2,659 [Hz] has two loops in which the both loops have the same direction on displacements. The fifth vibration mode in f_5 = 2,697 [Hz] also has two loops, but one loop moves in the opposite direction to the other one. Then, the sixth vibration mode has four large loops and one small loop in f_6 = 3,013 [Hz].

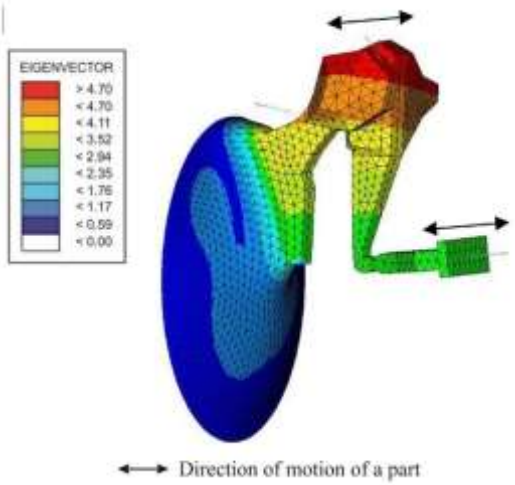

(a) Vibration mode of 1st natural frequency, f_1 = 1,033 [Hz]

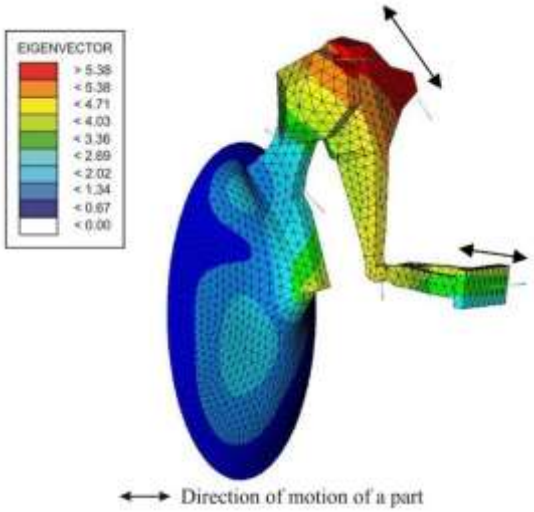

b) Vibration mode of 2nd natural frequency, f_2 = 1,728 [Hz]

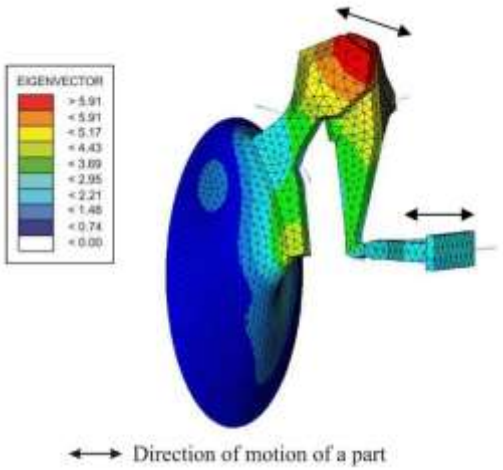

(c) Vibration mode of 3rd natural frequency, f_3 = 1,846 [Hz]

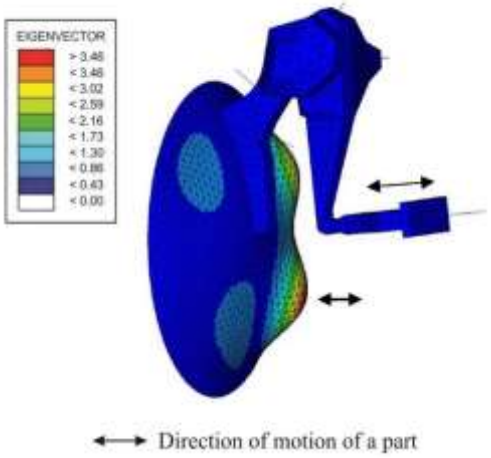

(d) Vibration mode of 4th natural frequency, f_4 = 2,659 [Hz]

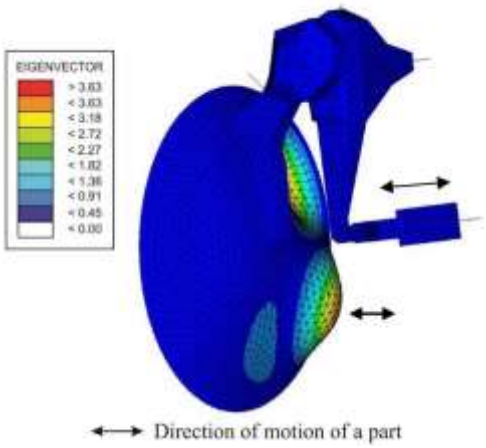

(e) Vibration mode of 5th natural frequency, f_5 = 2,697 [Hz]

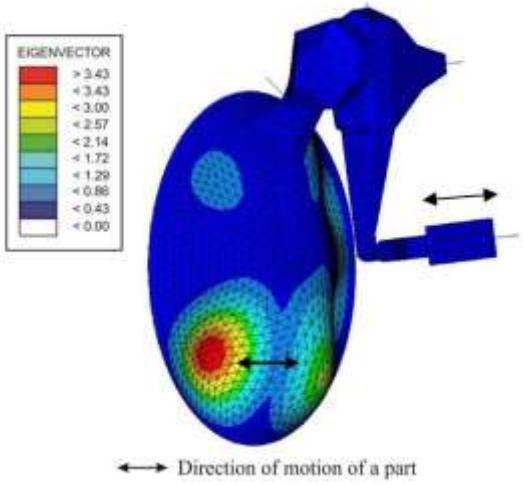

(f) Vibration mode of 6th natural frequency, f_6 = 3,013 [Hz]

Fig. 4.1 Vibration modes of the human ear system

4.4.2 Frequency Response Analysis

4.4.2.1 Calculation Method

Figure 4.2 shows the structural damping used for the human ear system using the structural damping coefficient of G = 0.4 in 1,500 [Hz] and less, and five kinds of values on G in 1,500 [Hz] and more. The Optistruct of Hypermesh was used to carry out the frequency response analyses of the human ear system using the torsional spring constant, $K_{\theta y} = 3.0 \times 10^{-5}$ [Nmm/rad] on the boundary under the sound pressure level, $P = 2.0 \times 10^{-5}$ [Pa] in the frequency range from 100 [Hz] to 10,000 [Hz]. Then five structural damping coefficients were used for the frequency response analyses to examine the effect of structural damping coefficients on the displacements of stapes in 1,500 [Hz] and more.

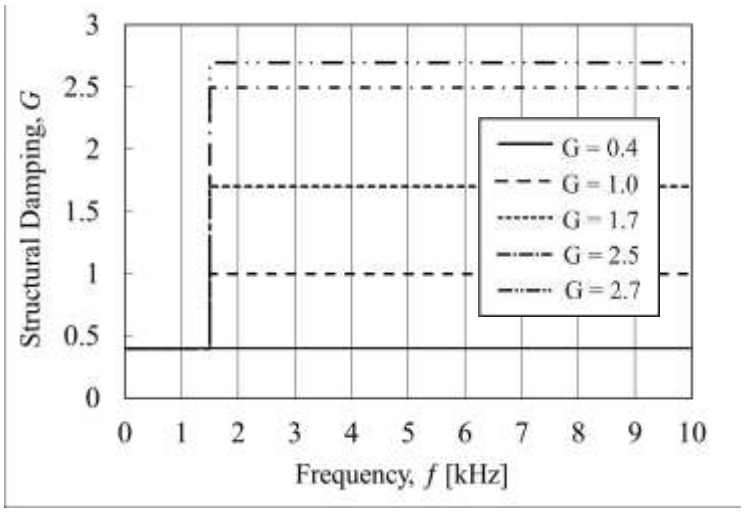

Fig. 4.2 Structural dampings used for the human ear system using structural damping coefficient of G = 0.4 in 1,500 [Hz] and less and five kinds of values on G in 1,500 [Hz] and more

4.4.2.2 Results

Figure 4.3 shows the frequency responses of displacements of the stapes of the human ear system. The use of structural damping coefficient of G = 0.4 can make the displacement constant at the frequency less than 1,000 [Hz]. However, The value of G = 0.4 makes the displacement very large in 1,500 [Hz] and more. Therefore, the frequency response analyses using five kinds of structural damping coefficients were carried out to decrease the large displacements in 1,500 [Hz] and more. Then, the value of G = 2.5 was selected as the structural damping coefficient in 1,500 [Hz] and more. Furthermore, it can be seen that the first natural frequency of the human ear system became around 1,000 [Hz]. It is well known that the first natural frequency of a human middle ear becomes around 1,000 [Hz] [22], [30]. Then, the frequency responses calculated in this study show the similar results reported by the other researchers [22], [44].

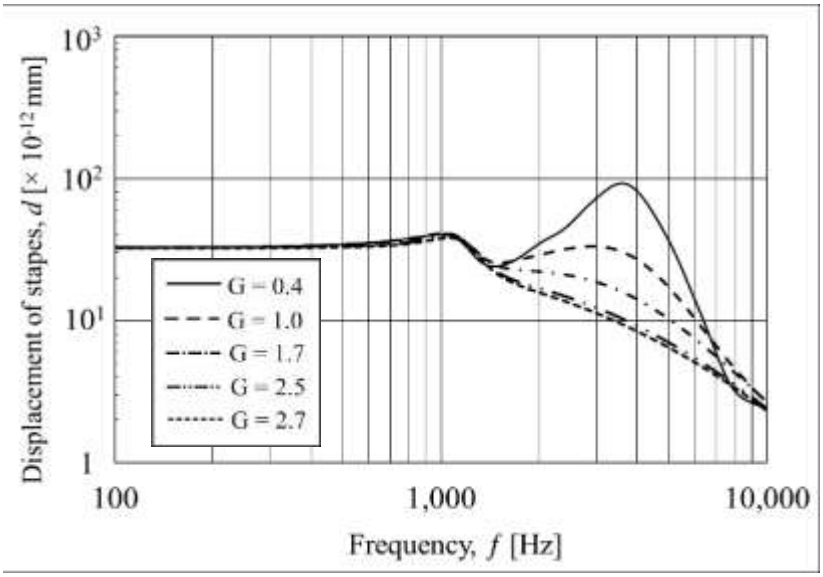

Fig. 4.3 Frequency response of the stapes displacement of the human ear system

4.4.3 Time History Response Analysis

4.4.3.1 Formant Frequencies on External Forces

4.4.3.1.1 Formant Frequencies

Formants are specific frequencies components of the acoustic signal produced by speech or singing. The information that humans require to distinguish between speech sounds can be represented purely by tube and chamber resonance. The formant with the lowest frequency is called F_1, the second F_2 and the third F_3. Most often the two first formants F_1 and F_2 are enough to distinguish the voice of vowel. Figure 4.4 shows the time history of the human vowel. The voices of vowels were recorded to obtain the time history of human vowel. Three types of voices of Japanese man, namely vowels "*a*", "*i*" and "*o*" were used. Then, the FFT (Fast Fourier Transform) was used to obtain the frequency response of human vowel.

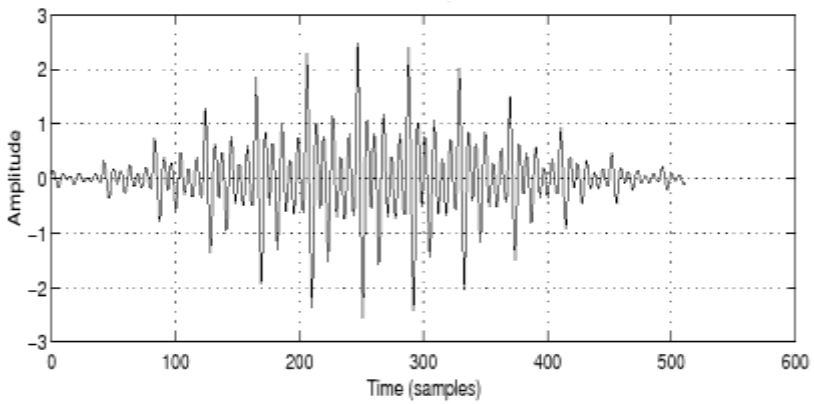

Fig. 4.4 Time history response of the human vowel

Figure 4.5 shows the frequency response of human vowel. In the frequency response of human vowel, three frequencies resonant or natural frequencies of human vowel were plotted. The F_1, F_2 and F_3 were first, second and the third Formants frequencies.

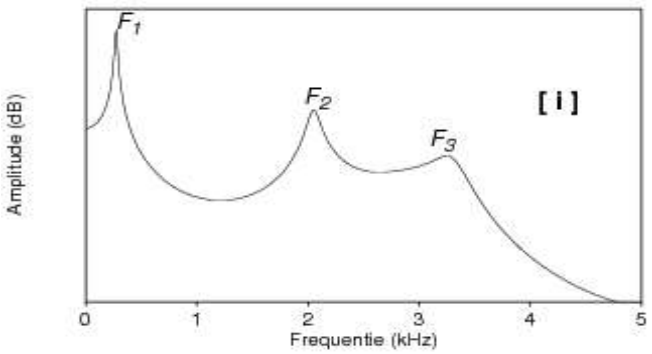

Fig. 4.5 Frequency response of human vowel

Figure 4.6 shows the Formant frequencies of Japanese man. The vertical and horizontal axis were the first Formant, F_1 and second Formant, F_2, respectively. The frequencies, F_1 = 750 [Hz], F_1 = 1,250 [Hz] and F_1 = 2,500 [Hz] are the first Formant frequencies of “o”, “a” and “i” ,respectively used in the time history response analysis of human ear system.

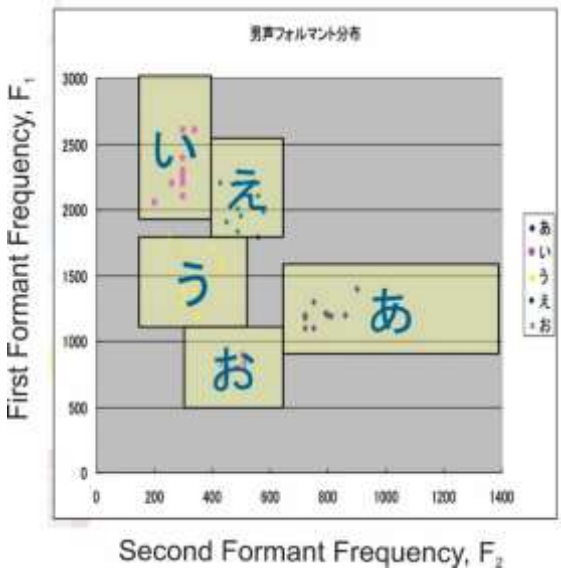

Fig. 4.6 Formant frequencies of Japanese man

4.4.3.1.2 Calculation Method

The Optistruct of HyperMesh was used to carry out time history responses analyses of human ear system. The value of $P = 2.0 \times 10^{-6}$ [Pa] was used as the external pressure subjected to the eardrum. As for the frequencies of the external pressure, the Formant frequencies were used. The frequencies, $F_1 = 750$ [Hz], $F_1 = 1{,}250$ [Hz] and $F_1 = 2{,}500$ [Hz] are the first Formant frequencies of "*o*", "*a*" and "*i*" in human simple vowels, respectively. Then as for the structural damping coefficients, G, the values of $G = 0.4$ and G = 2.5 were used in 1,500 [Hz] and less, and in 1,500[Hz] and more, respectively. As for the incremental time, Δt and the number of time, N, $\Delta t = 1.0 \times 10^{-5}$ [s] and $N = 800$ were used, respectively.

4.4.3.1.3 Results

Figure 4.7 shows the time history responses of displacements in the stapes of human ear system when the eardrum was subjected to the external pressure, $P = 2.0 \times 10^{-6}$ [Pa] consisting of the Formant frequencies of human voice. It can be seen that the time history responses using the Formant frequencies, $F_1 = 750$ [Hz] and $F_1 = 1{,}250$ [Hz] have almost the same displacements. Otherwise, the time history response using the Formant frequency, $F_1 = 2{,}500$ [Hz] has smaller displacements than the others. It must be due to that the large structural damping coefficient, $G = 2.5$ was used in 1,500 [Hz] and more.

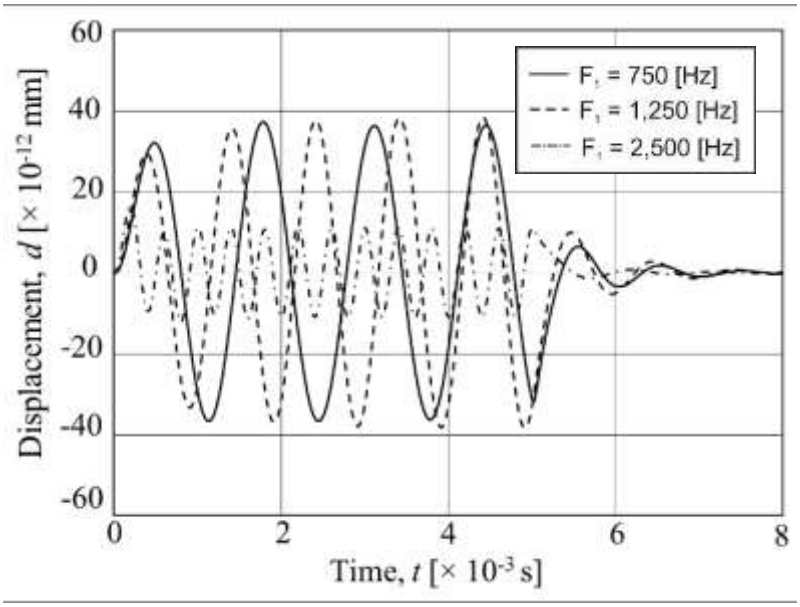

Fig. 4.7 Time history responses of displacements in the stapes of human ear system when the eardrum was subjected to the external pressure, $P = 2.0 \times 10^{-5}$ [Pa] consisting of the Formant frequencies of human voice

4.4.3.2 Human Voices as External Forces

4.4.3.2.1 Original Human Voices Downloading From Website

Figure 4.8 shows the time histories of original sound pressures downloaded from the website opening samples of human voices as wav files (http://www.geocities.jp/onsei2007/wav_data51/wav_data 51.html). Firstly, the downloaded human voices such as "*i*", "*u*" and "*e*" were converted to csv files using Scilab. Each human voice has a single channel, namely a mono sound in 0.25 [s].

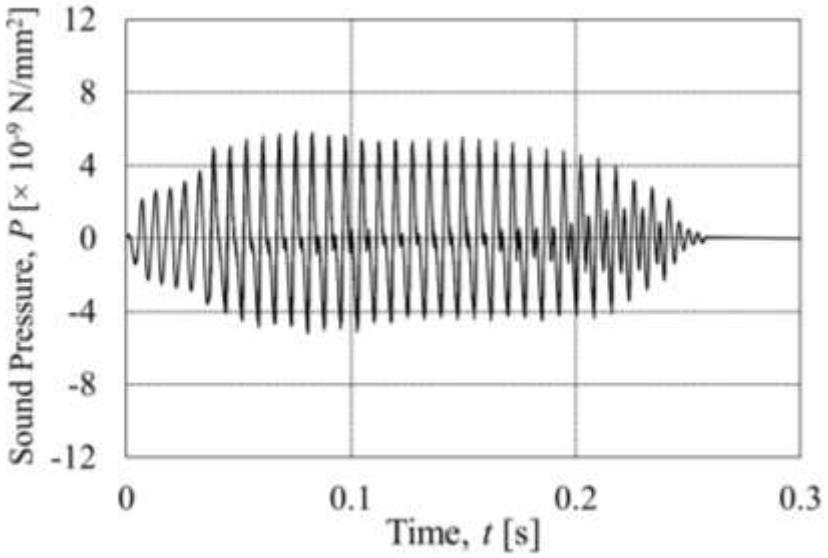

(a) Original sound pressure on vowel "*i*"

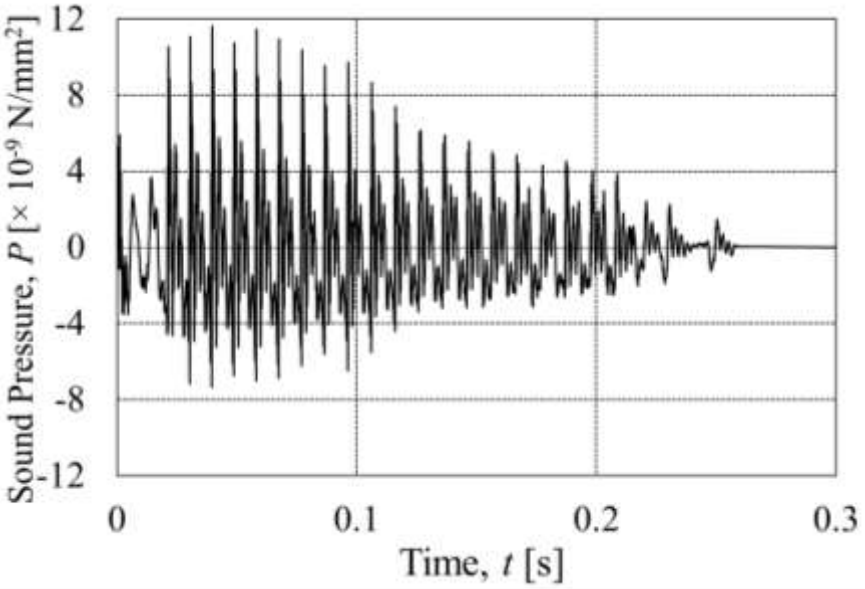

(b) Original sound pressure on vowel "*u*"

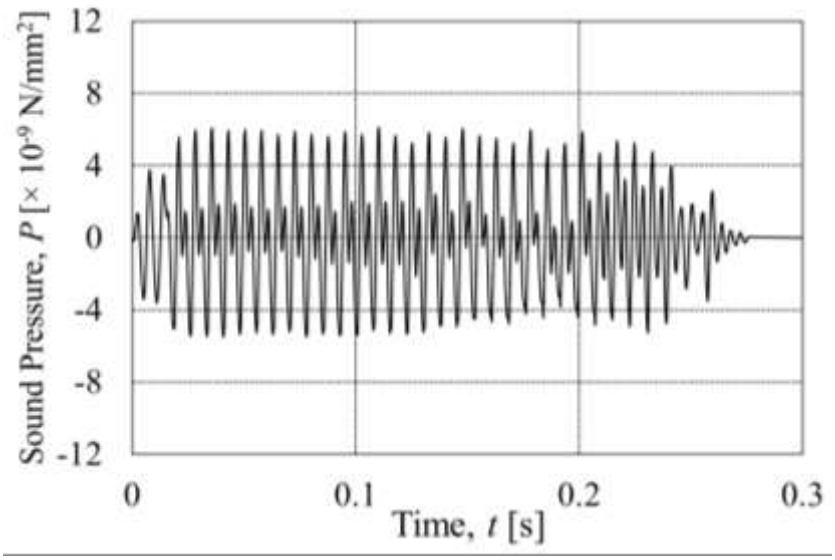

(c) Original sound pressure on vowel “e”

Fig. 4.8 Time histories of original sound pressures downloaded from a website opening samples of human voices as wav files (http://www.geocities.jp/onsei2007/wav_data51/wav_data51.html)

4.4.3.2.2 Creating Input Sound Pressures

Two types of sounds were created by using the downloaded original sound pressures. The first type of sounds are the sound pressures in 0.022[s] to use as input data, namely external forces in Hypermesh. The second type of them are the sound pressures in 2[s] to evaluate the sounds by listening them. Figure 4.8 shows the time histories of sound pressures in 0.02[s] created by connecting three basic waveforms so that they may not exceed the limitation of input data in Hypermesh. As for the second type of sounds, they were created as data in 2[s] so that the authors can evaluate them, by the same method as the first type of them. The waveforms of created sound pressures on vowel “*e*” are a little more complex than vowels “*i*” and “*u*”.

Figure 4.9 shows the evaluation of differences among the original sounds, the sounds in 2[s] created as input data of Hypermesh and the sounds in 2[s] created by using the results calculated by Hypermesh. The created sound pressures of csv files were converted to wav files by using Scilab. Then, the original sounds and the sounds in 2[s] created in the same way as input data of Hypermesh of wav files were played in order to evaluate them before using them as input data of Hypermesh. Then, the original sounds and the created sounds were compared for each vowel. The results of evalutions showed that the created sounds on vowels "*i*", "*u*" and "*e*" were identical to its original sounds. Therefore, the created sounds as input data for the three vowels were feasible to input them into the Hypermesh in order to carry out the time history response analysis of the human ear system.

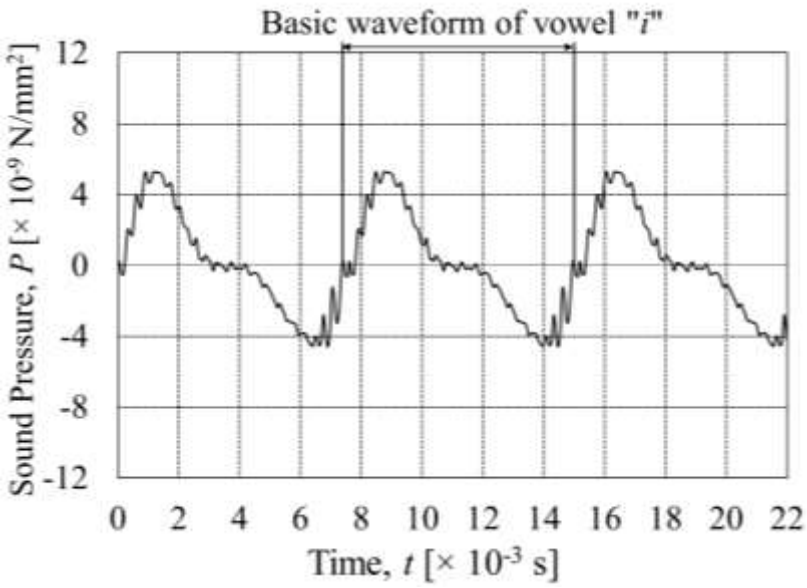

(a) Created sound pressure on vowel "*i*"

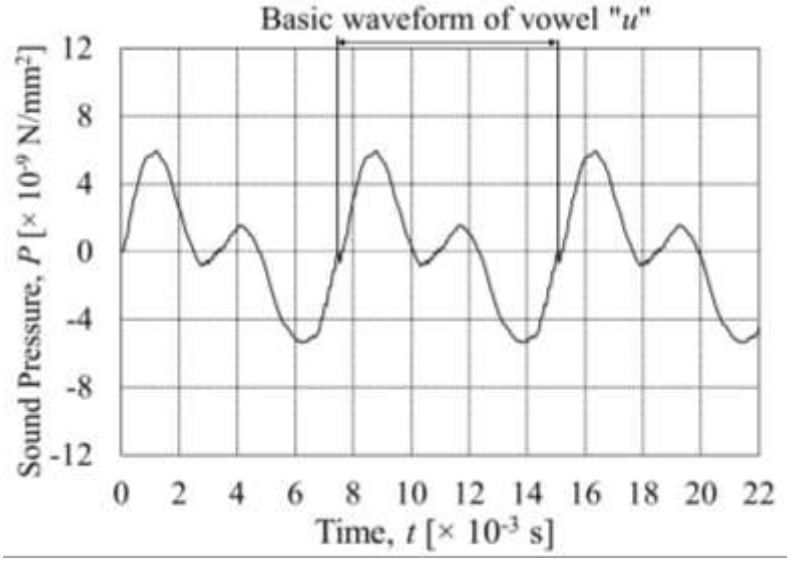

(b) Created sound pressure on vowel “u”

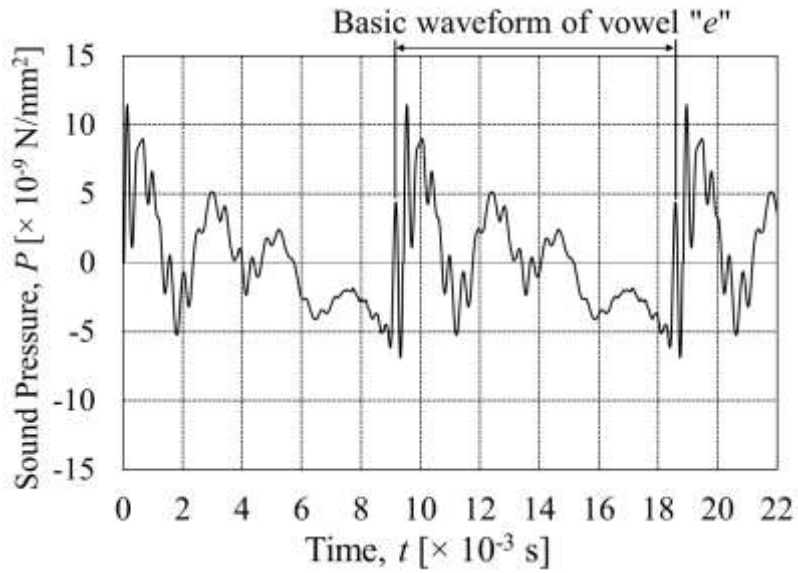

(c) Created sound pressure on vowel “*e*”

Fig. 4.8 Time histories of sound pressures in 0.022[s] created by connecting three basic waveforms so that they may not exceed the limitation of input data in Hypermesh

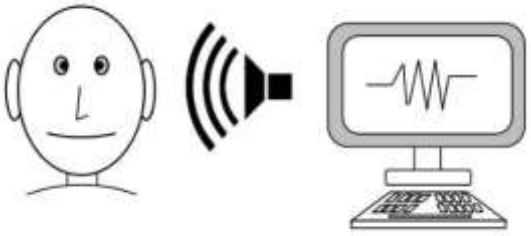

Fig. 4.9 Evaluation of differences among the original sounds, the sounds in 2[s] created as input data of Hypermesh and the sounds in 2[s] created by using the results calculated by Hypermesh.

The Optistruct in HyperWorks was used to carry out time history responses analysis of human ear system. The sound pressure in 0.022[s] on vowel "*i*", "*u*" or "*e*" created for input data was load to the eardrum of human ear system as the external force. Then, as for the structural damping coefficients, G, the values of $G = 0.4$ and $G = 2.5$ were used in 1,500 [Hz] and less, and in 1,500 [Hz] and more, respectively. As for the incremental time, Δt and the number of time, N, $\Delta t = 1.0 \times 10^{-4}$ [s] and $N = 220$ were used, respectively.

4.4.3.2.3 Results

Figure 4.10 shows the calculated time history responses of displacements at the stapes when the eardrum was subjected to the created sound pressures. In comparison between the created input data shown in Figure 4.8 and the calculated output ones shown Figure 4.10, it is understood that high frequency components of the calculated output data reduce due to an effect of the structural damping.

The sounds in 2[s] created by using the calculated output data of csv files were converted to wav files by using Scilab. Then both the sounds in 2[s] created in the same way as the created input data and the sounds in 2[s] created by using the calculated

output ones of wav files were played in order to evaluate them. The evaluation of differences between both the sounds in 2[s] was carried out as shown in Figure 7. In the results of evaluation, it was obtained that the sounds of calculated output data could be heard more clearly than those of the created input ones because the high frequency components of calculated output data reduced due to the effect of the structural damping.

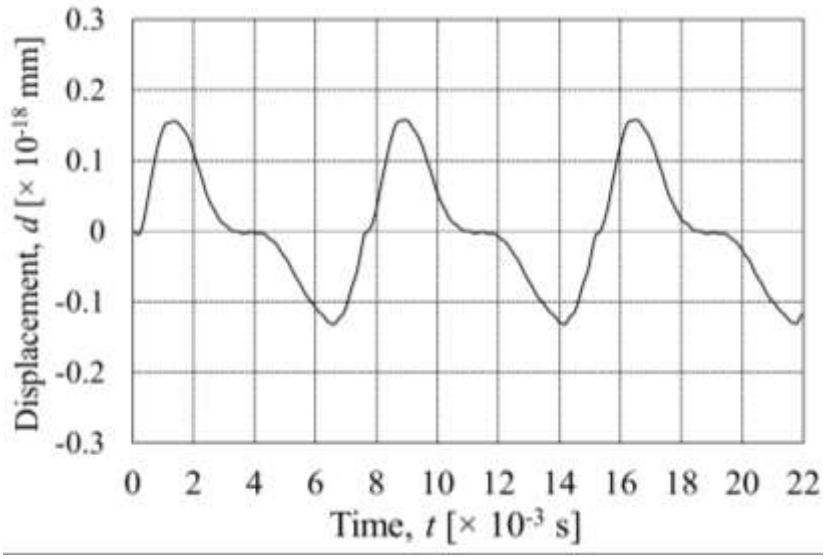

(a) Displacement for vowel "*i*"

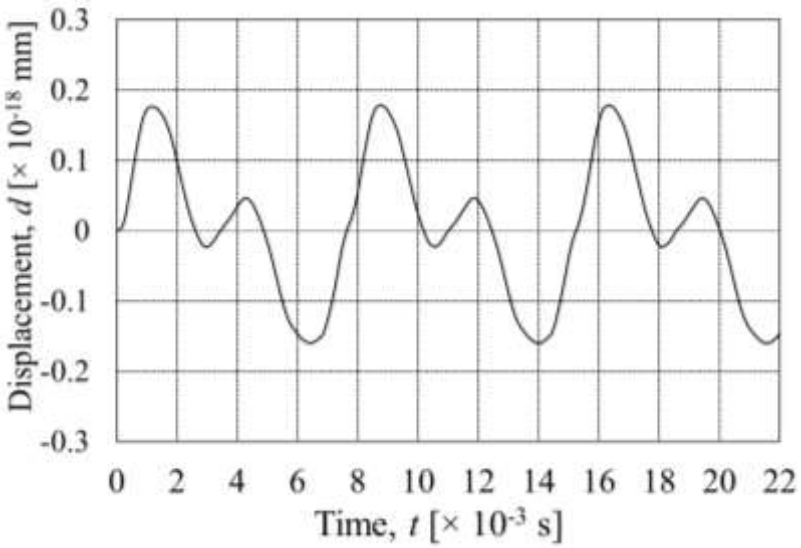

(b) Displacement for vowel "*u*"

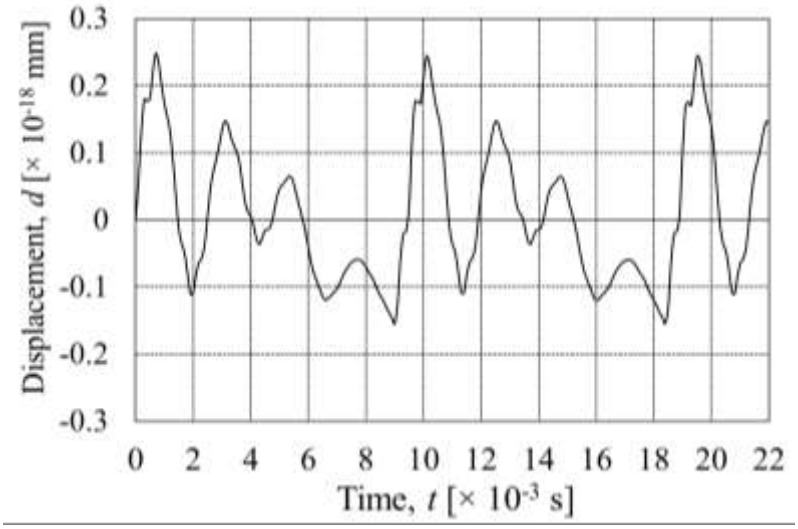

(c) Displacement for vowel "*e*"

Fig. 4.10 Calculated time history responses of displacements at the stapes when the eardrum was subjected to the created sound pressures

4.5 Human Ear System Using Boundary Modeled with Finite Elements Considering Four Types of Eardrums

Figure 4.11 shows the example finite element models of human ear systems containing a middle ear, a cochlea in inner ear, four ligaments, a tendon and a tensor tympanic membrane. As for the human ear systems, each human ear system includes each eardrum in the four types of eardrums. The ligaments, tendon and tensor tympanic membrane were considered as translational springs. The shapes and dimensions of the three ossicles were decided by considering the references [29],[43]. Then, the CAD software (solidworks 2015) was used to create the three dimensional model of the human ear systems. The eardrums and the three ossicles were meshed by using six-node triangular elements and ten-node tetrahedron elements, respectively.

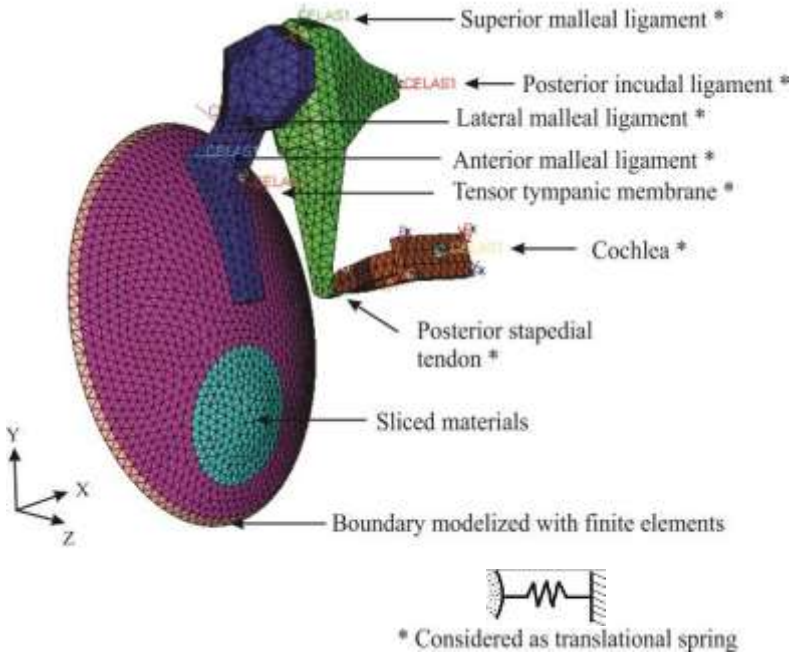

Fig. 4.11 Example of finite element models of human ear systems containing a middle ear, a cochlea in an inner ear, four ligaments, a tendon and a tensor tympanic membrane

Table 2 shows the material properties of ossicles. The values in table 2 were decided considering the author's previous published [22].

Table 2. Material properties of ossicles

Structure	Young's modulus [$\times 10^9$ [N/m^2]]	Mass density [$\times 10^3$ kg/m^3]	Poisson's ratio [-]*
Malleus	14	2.55	0.3
Incus	14	2.36	0.3
Stapes	14	2.20	0.3

*[-] means a dimensionless quantity

Table 3 shows the translational springs constants of ligaments, a tendon, a tensor tympanic membrane and a cochlea. As for the ligaments, the tendon and the tensor tympanic membrane, each of them was considered as three translational springs in *x, y* and *z* directions. The indexes, *x*, *y* and *z* of each spring constant denote the local coordinates of itself. The *x*-direction of each local coordinate frame was defined in the

normal direction to the surface of an ossicle. The values of translational spring constants, K_i ($i = x, y, z$) for the ligaments, the tendon, the tensor tympanic membrane and the cochlea were decided by trial and error so that the stapes can perform a piston motion in the x-direction of local coordinate frame. The stapes contacting with the cochlea moves like a piston in the x-direction. As for the boundary of the eardrums, the boundary modeled with finite elements was used as boundary condition of the eardrums.

Table 3. Translational springs constants of ligaments, a tendon, a tensor tympanic membrane and a cochlea

Component	Spring constant, K_x [N/mm]	Spring constant, $K_y = K_z$ [N/mm]
Anterior malleal ligament	1.2	0.3
Lateral malleal ligament	1.2	0.3
Superior malleal ligament	1.2	0.3
Posterior incudal ligament	1.2	0.3
Tensor tympanic membrane	1.2	0.3
Posterior stapedial tendon	1.2	0.3
Cochlea	0.2	-

4.5.1 Frequency Response Analysis

4.5.1.1 Calculation Method

The frequency response analysis was performed to compare the responses of the four types of human ear systems under the sound pressure level, $P = 2.0 \times 10^{-5}$ [Pa]. The Optistruct of Hypermesh was used to carry out the frequency response analysis in the

frequency range 100 to 10,000 [Hz]. The structural damping coefficients of G = 0.4 for less than 1500 [Hz] and G = 2.5 for more than 1500 [Hz].

4.5.1.2 Results

Figure 4.12 shows the frequency responses of the four types of human ear systems. The human ear system using eardrum with a hole has the lowest displacement in low and high frequency. Then, the displacement of the human ear system using the eardrum repaired by the sliced material with thickness, t = 0.1 [mm] having the same material properties as the eardrum was approaching the displacement of human ear system using the normal eardrum rather than the human ear system using the eardrum repaired by the slice cartilage in low and medium frequencies. Otherwise, in the high frequency, the use of sliced cartilage with thickness, t = 0.4 [mm] was better than sliced material.

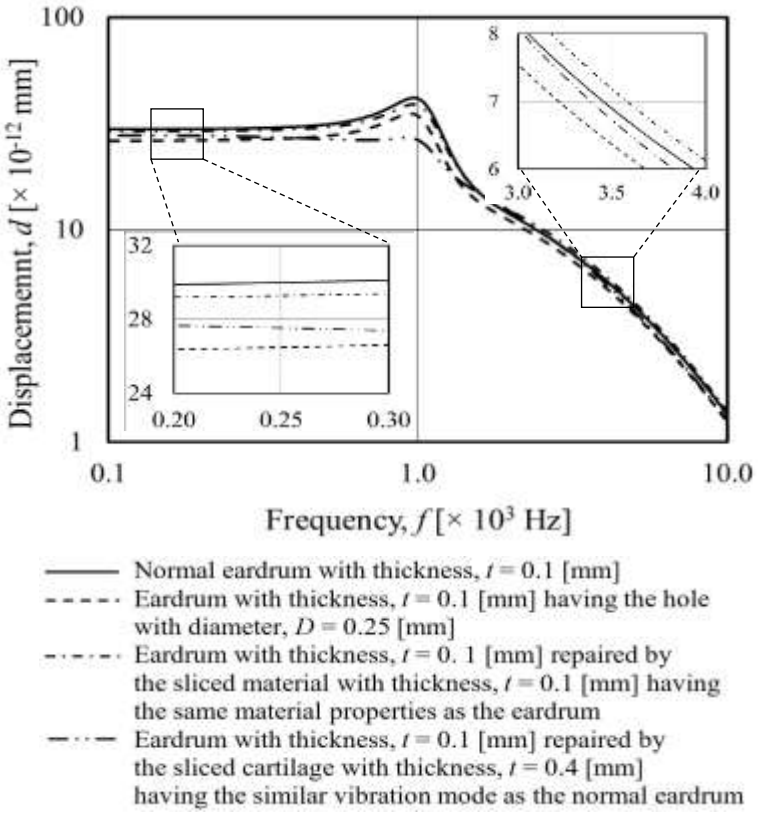

Fig. 4.12 Frequency responses of the four types of human ear systems

4.5.2 Time History Response Analysis

4.5.2.1 Calculation Method

Figure 4.13 shows the time history of sound pressure created by connecting three basic waveforms of vowel "*i*" downloaded from a website opening samples of human voices as wav files. The solver of Hypermesh namely Optistruct was used to carry out time history response analysis of the four types of human ear systems. In this analysis, the human voices created as input sound pressure were used as the external forces. The sound pressure in 0.022 [s] on vowel "*i*" created for input data was loaded to the eardrums of human ear systems. Then, the structural damping coefficient, $G = 0.4$ and $G = 2.5$ were used in 1500 [Hz] and less, and in 1500 [Hz] and more, respectively. As for the incremental time, Δt and the number of time, N, $\Delta t = 1.0 \times 10^{-4}$ [s] and $N = 220$ were used, respectively.

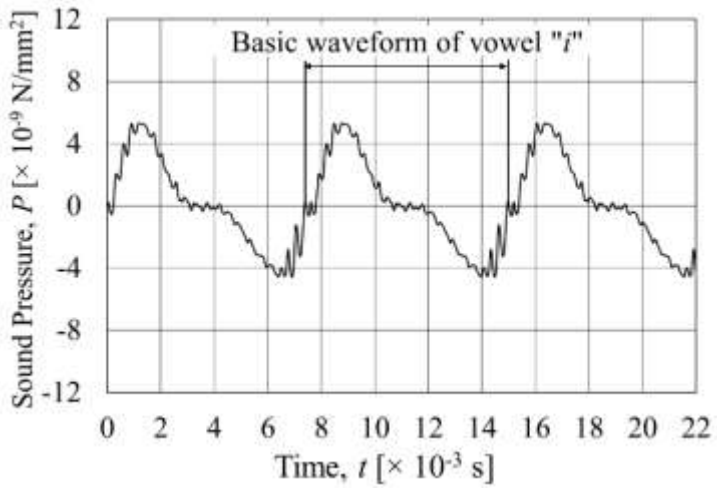

Fig. 4.13 Time history of sound pressure created by connecting three basic waveforms of vowel "*i*" downloaded from a website opening samples of human voices as wav files

4.5.2.2 Results

Figure 4.14 shows the time history responses of the four types of human ear systems when the eardrums were subjected to the human voice by using the created sound pressure of vowel "*i*". The human ear system using the eardrum with a hole has the lowest displacement among the four types of the human ear systems. As for the human ear system using eardrum repaired by the sliced cartilage with thickness, t = 0.4 [mm] and the sliced material with thickness, t = 0.1 [mm] having the same material properties as the eardrum, the displacement of the human ear system using eardrum repaired by the sliced material was approaching the human ear system using normal eardrum with thickness, t = 0.1 [mm]. Then, the use of sliced material having the same material properties as the eardrum may be required.

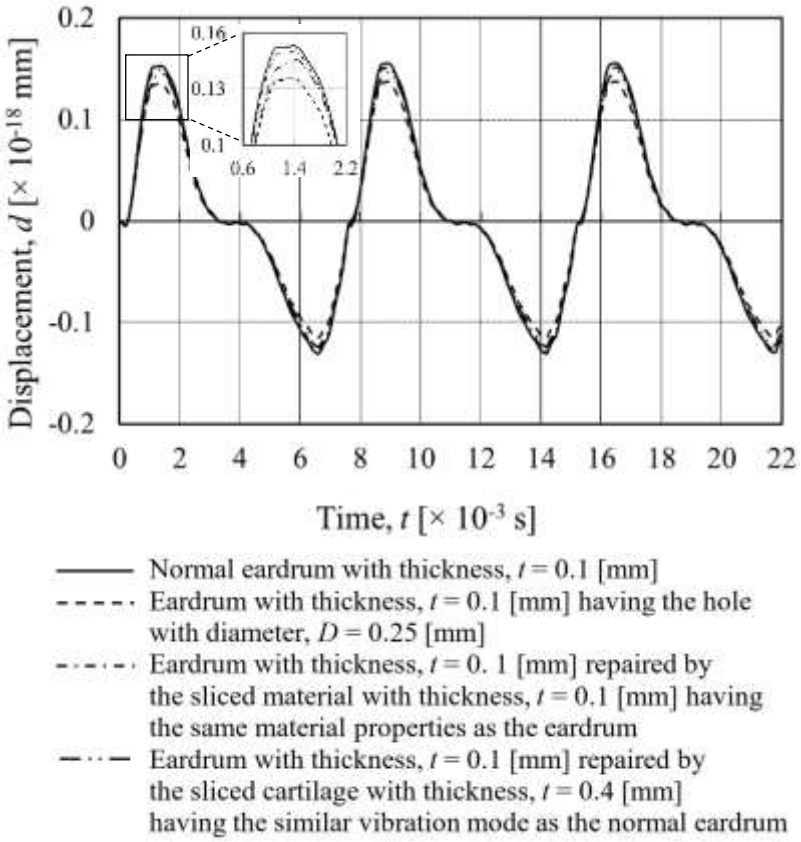

Fig. 4. 14 Time history responses of the four types of human ear systems when the eardrums were subjected to the human voice by using the created sound pressure of vowel "*i*"

4.6 Conclusions

The summary of results is shown below.

1. The eigen-value, frequency response and time history response analyses of human ear system using torsional springs as boundary condition as boundary condition had been carried out.
2. It was obtained that the sounds of calculated data could be heard more clearly than those of created input ones in time history response analysis using human voices as the external forces because the high frequency components of the calculated output data reduced due to the effect of the structural damping.
3. It was shown that the frequency responses and time history responses of the human ear system using the sliced cartilage were lower than those of the sliced material having the same material properties as a human eardrum due to the increase of mass of the sliced cartilage. The material having the same material properties as the eardrum extracted from human body instead of the sliced cartilage used currently in myringoplasty may be required.

Chapter 5

Conclusions

The summary of the results of a study on finite element dynamics of human ear system containing middle ear, cochlea in inner ear, ligaments, tendon and tensor tympanic membrane is shown below.

1. The three-dimensional modeling of human ear system to perform dynamic analyses, namely eigen-value, frequency response and time history response analyses using finite element method had been developed in this study.
2. The eigen-value analyses of the human ear systems and the four types of eardrums, namely normal eardrum, eardrum with hole, eardrum repaired by sliced cartilage and eardrum repaired by sliced material having the same material properties as human eardrum were performed using finite element method. It was determined that the proper thicknesses of the sliced cartilage were from 0.4 [mm] to 0.45 [mm] and the sliced material was 0.1 [mm] by comparing the vibration modes and natural frequencies of the four types of eardrums.
3. Frequency response and time history response analyses with formant frequencies as frequencies of external forces and human voices as the input sound pressures were performed in this study. In the time history response analysis with human

voices as input sound pressures, it was obtained that the sounds calculated output data could be heard more clearly than those of the created input once because the high frequency components of the calculated output data reduced due to the effect of the structural damping.

References

[1] Wada, H., Kobayashi, T., Naganuma, H. & Tachizaki, H (1990) Analysis of Dynamic Characteristics of Eardrum (Young's Modulus, Thickness and Damping Ratio of Human Eardrum). *Japan Society of Mechanical Engineers,* 56, 87-90.

[2] Funnel, W.R. J. and Lazlo, C. A. (1978) Modelling of the cat eardrum as a thin shell using finite element method, J. Acoust. Soc. Am. 63, 1461-1467.

[3] De Graf, D., Aernouts, J., Aerts, J., Cheng, J.T., Horwitz, R., Rosowski, J.J. & Dirckx, J.J. (2014) Viscoelatic properties of the human tympanic membrane studied with stroboscopic holography, *Hearing Research,* 312, 69-80.

[4] Skordzka, E. and Modlawska, J. (2006) Modal analysis of the human tympanic membrane of middle ear using the finite-element method, *Archieves Of Acoustics* 31, 23-28.

[5] Greef, D.D., Goyens, J., Pintelon, I., Bogers, J.P., Rompaey, V.V., Hamans, E., Heyning, P.V. & Dirckx, J.J.J. (2016) On the Connection Between the Tympanic Membrane and the Malleus, *Hearing Research,* 340, 50-59.

[6] Gentil, F., Parente, M., Martins, P., Garbe, C., Santos, C., Areias, B., Branco, C., Paco, J. & Jorge, R.N. (2016). Effects of the Fibers Distribution in the Human Eardrum : A Biomechanical Study, *Journal of Biomechanics*, 49, 1518-1523.

[7] Zhang, X. & Gan, R.Z. (2012) Dynamic Properteis of Human Tympanic Membrane Based on Frequency-Temperature Superposition. *Annals of Biomedical Engineering,* 41, 205-214.

[8] Wu, C., Chen, Y, Al-Furjan, M.S.H., Ni, J. & Yang, X. (2016) Free Vibration Model and Theoretical Solution of the Tympanic Membrane, *Computer Assisted Surgery,* 21, 62-69.

[9] Dirckx, J.J.J. & Decraemer, W.F. (1991) Human Tympanic Membrane Deformation Under Static Pressure, *Hearing Research,* 51, 93-106.

[10] Mehta, R.P., Rosowski, J.J., Voss, S.E., O'Neil, E. & Merchant, S.N. (2006) Determinants of Hearing Loss in Perforations of the Tympanic Membrane, *Otology & Neurotology,* 27, 136-143.

[11] Voss, S.E., Rosowski, J.J., Merchant, S.N. & Peake, W.T. (2001) Middle Ear Function with Tympanic Membrane Perforations, *Journal Acoustical Society of America,* 110(3), 1445-1452.

[12] Saliba, I., Abela, A. & Arcand, P. (2011) Tympanic Membrane Perforation : Size, Site and Hearing Evaluation. *International Journal of Pediatric Otorhinolaryngology,* 75, 527-531.

[13] Zahnert, T., Huttenbrink, K.B., Murbe, D. & Bornitz, M. (2000) Experimental Investigations of the Use of Cartilage in Tympanic Membrane Reconstruction, *The American Journal of Otology,* 21, 322-328.

[14] Murbe, D., Zahnert, T., Bornitz, M., Huttenbrink, K.B. (2002) Acoustic Properties of Different Cartilage Reconstruction Technique of the Tympanic Membrane, *The Laryingoscope,* 112, 1769-1776.

[15] Aarnisalo, A.A., Cheng, J.T., Ravicz, M.E, Hulli, N., Harrington, E.J., Montes, M.S.H., Furlong, C., Merchant, S.N. & Rosowski, J.J. (2009) Middle Ear Mechanics of Cartilage Tympanoplasty Evaluated by Laser Holography and Vibrometry, *Otology & Neurotology,* 30, 1209-1214.

[16] Jiang, H., & Zhang, Z. (2014). Cartilage Tends to be a Better Choice than Temporalis Fascia for Tympanoplasty under the Circumstance of Eustachian Tube Dysfunction, *Annals of Otolorayngology and Rhinology*, 1(3).

[17] Tek, A., Karaman, M., Uslu, C., Habesoglu, T., Kihcarslan, Y., Durmus, R., Esen, S. & Egeli, E. (2011) Audiological and Graft Take Result of Cartilage Reinforcement Tympanoplasty (a new technigque) versus Fascia, *Eur Arch Otorhinolaryngol*.

[18] Allardyce, B.J., Rajkhowa, R., Dilley, R.J., Xie, Z., Campbell, L., Keating, A., Atlas, M.D., Unge, M.v. & Wang, X. (2016) Comparative Acoustic Performance and Mechanical Properties of Silk Membranes for the Repair of Chronic Tympanic Membrane Perforations. *Journal of the Mechanical Behavior of Biomedical Materials*, 64, 65-74.

[19] Dornhoffer, J.L. (1997) Hearing Results with Cartilage Tympanoplasty, *The Laryngoscope,* 107, 1094-1099.

[20] Lee, C.F., Hsu, L.P., Chen, P.R., Chou, Y.F., Chen, J.H. & Liu, T.C. (2006) Biomechanical Modeling and Design Optimization of Cartilage Myringoplasty Using Finite Element Analysis. *Journal Audiology & Neurotology,* 11, 380-388.

[21] Lee, C.F., Chen, J.H.C., Chou, Y.F., Hsu, L.P., Chen, P.R. & Liu, T.C. (2007) Optimal Graft Thickness for Different Sizes of Tympanic Membrane Perforation in Cartilage Myringoplasty : A Finite Element Analysis, *The Laryngoscope*, 117, 725-730.

[22] Koike, T. & Wada, H. (2002) Modelling of the human middle ear using the finite element method, *Journal Acoustical Society of America,* 111 (3), 43-64.

[23] Beer, H.J., Bornitz, M., Hardtke, H.J., Schmidt, R., Hofman, G., Vogel, U. & Zahnert, T., Huttenberk, K.B. (1998). Modeling of Components of the Human Middle Ear and Simulation of Their Dynamic Behaviour. *Audiol Neurotol*, 4, 156-162.

[24] Greef, D.D., Pires, F. & Dirckx, J.J.J. (2017) Effects of Model Definitions and Parameter Values in Finite Element Modeling of Human Middle Ear Mechanics, *Hearing Research,* 344, 195-206.

[25] Bornitz, M., Hardtke, H.J. & Zahnert, T. (2010). Evaluation of Implantable Actuators by Means of a Middle Ear Simulation Model, *Hearing Research,* 263, 145-151.

[26] Wang, X., Cheng, T. & Gan, R.Z. (2007) Finite Element Analysis of Middle Ear Pressure Effects on Static and Dynamic Behavior of Human Ear, *Journal Acoustical Society of America,* 122(2), 906-917.

[27] Wada, H. & Metoki, T. (1992) Analysis of Dynamic Behavior of Human Middle Ear Using Finite Element Method, *Journal of Acoustical Society of America,* 92, 3157-3168.

[28] Ferris, P. & Prendegast, P.J. (2000) Middle Ear Dynamics Before and After Ossicular Replacement, *Journal of Biomechanics,* 33, 581-590.

[29] Liu, Y., Li, S. & Sun, X. (2009) Numerical analysis of ossicular chain lesion of human ear, *Acta Mechanica Sinica,* 25, 241-247.

[30] Lee C.F, Chen, P.R., Lee, W.J., Chen, J.H. & Liu, T.C. (2006) Computer aided three dimensional reconstruction and modelling of middle ear biomechanics by high-resolution computed tomography and finite element analysis, *Biomedical Engineering, Basis & Communications*, 188, 214-221.

[31] Gan, R.Z., Feng, B. & Sun, Q. (2004) Three-dimensional finite element modelling of human ear for sound transmission, *Annals of Biomedical Engineering*, 32, 847-859.

[32] Sun, Q., Gan, R.Z., Chang, K.H. & Dormer, K,J. (2002). Computer Integrated Finite Element Modeling of Human Middle Ear. *Biomechan Model Mechanobiol*, 1, 109-122.

[33] Gan, R.Z., Sun, Q., Dyer, R.K., Chang, K.H. & Dormer, K.J. (2002). Three Dimensional Modeling of Middle Ear Biomechanics and Its Applications, *Otology & Neurology*, 23, 271-280.

[34] Wang, X., Hu, Y., Wang, Z. & Shi, H. (2011). Finite Element Analysis of The Coupling Between Ossicular Chain and Mass Loading for Evaluation of Implantable Hearing Device. *Hearing Research*, 280, 48-57.

[35] Spiridon, I.F., Sakellarios, A.I., Rigas, G.A., Tagaris, A., Bellos, C.V., Bibas, A., Bohnke, F., Iliopuolou, D., Koutsouris, D. & Fotiadis, D.I. (2015) Effect of Modeling Parameters on the Frequency Response of the Middle Ear by Means of Finite Element Analysis. *Proceeding of Annual International Conference of the IEEE Engineering in Medicine and Biology Society, EMBS,* 7318514, 925-928.

[36] Kasmitcheff, G., Miroir, M., Nguyen, Y., Ferray, E., Sterkers, O., Cotin, S., Duriez, C. & Grayeli, A.B. (2014) Validation Method of a Middle Ear Mechanical Model to Develop a Surgical Simulator, *Audiology & Neurotology,* 19, 73-84.

[37] Gentil, F., Parente, M., Martins, P., Garbe, C., Paco, P., Ferreira, A.J.M., Travers, J.M. & Jorge R.N (2013) The Influence of Muscles Activation on the Dynamical Behaviour of the Tympano-Ossicular System of the Middle Ear, *Computer Method in Biomechanics and Biomedical Engineering,* 16, 392-402.

[38] Gan, R.Z., Zhang, X. & Guan, X. (2011) Modeling Analysis of Biomechanical Changes of Middle Ear and Cochlea in Otitis Media, *American Institute Physics Conference Proceedings,* 1403, 539-544.

[39] Nie, X., Lui, H., Huang, X., Tan, J., Xie, X., Yao, W., Rao, Z. & Duan, M. (2011) Finite Element Model of Human Ear Reconstruction Through Micro-Computer Tomography, *Acta Oto-Laryngologica*, 131, 269-276.

[40] Gentil, F., Parente, M., Martins, P., Garbe, C., Jorge, P., Ferreira, A.J.M., Travers, J.M. (2010) The Influence of the Mechanical Behaviour of the Middle Ear Ligaments : a Finite Element Analysis, *Proceeding of the Institution of Mechanical Engineers, Port H : Journal of Engineering in Medicine*, 225(1), 68-76.

[41] Liu, H., Rao, Z. & Ta, N. (2010) Finite Element Analysis of the Effects of a Floating Mass Transducer on the Performance of a Middle Ear Implant. *Journal of Medical Engineering & Technology,* 34(5-6), 316-323.

[42] Hoffstetter, M., Schardt, F., Lenarz, T., Wacker, S. & Wintermantel, E. (2010) Parameter Study on a Finite Element Model of the Middle Ear, *Biomedical Technology,* 55, 19-26.

[43] Bohnke, F., Bretan, T., Lehner, S. & Strenger, T. (2013) Simulations and measurements of human middle ear vibrations using multi-body systems and laser doppler vibrometry with the floating mass tranducer, *Materials*, 6, 4675-4688.

[44] Sun, Q., Chang, K.H., Dormer, K.J., Dyer, R.K.Jr. & Gan, R.Z. (2002) An advanced computer-aided geometric modeling and fabrication for human middle ear, *Medical Engineering & Physics,* 2, 595-606.

[45] Ahn Tae-Soo, et al, Experimental measurement of tympanic membrane response for finite element model validation of a human middle ear, *Springer Plu*s 2, 527, 2013.

[46] Volandri, G, Puccio, D.F., Forte, P. & Manetti, S. (2012). Model-Oriented Review and Multi-Body Simulation of the Ossicular Chain of the Human Middle Ear, *Medical Engineering & Physics,*34, 1339-1355.

[47] Decraemer, W.F., Dirckx, J.J.J., & Funnel, W.R.J. (2003) Three-Dimensional Modelling of the Middle-Ear Ossicular Chain Using a Commercial High-Resolution X-Ray CT Scanner, *Journal of the Association for Research in Otolaryngology*, 04, 250-263.

[48] Kovincic, N.I. & Spasic, D.T. (2016) Dynamics of a Middle Ear with Fractional Type of Dissipation. *International Journal of Nonlinear Dynamics and Chaos in Engineering Systems,* 85, 2369-2388.

[49] Rusinek, R., Warminski, J., Szymanski, M., Kecik, K. & Kozik, K. (2016) Dynamics of the Middle Ear Ossicles with a SMA Prosthesis, *International Journal of Mechanical Science.*

[50] Greef, D.D., Buytaert, J.A.N., Aerts, J.R.M., Hoorebeke, L.V., Dierick, M. & Dirckx, J. (2015) Details of Human Middle Ear Morphology Based on Micro-CT Imaging of Phosphotungstic Acid Stained Samples, *Journal of Morphology,* 276, 1025-1046.

[51] Qi, L., Funner, W.R.J., Daniel, S.J. (2008) A Nonlinear Finite-Element Model of the Newborn Middle Ear, *Journal Acoustical Society of America*, 124(1), 337-347.

[52] Higashimachi, T., Shiratake, Y., Maeda, T., Sug, K. & Toriya, R. (2013) Three Dimensional Finite Element Analysis of the Human Middle Ear and an Application for Clinics Tympanoplasty, *Surface Effect and Contact Mechanic,* 78, 61-72.

[53] Gan, R.Z., Reeves, B.P., & Wang, X. (2007) Modeling of Sound Transmission from Ear Canal to Cochlea. *Annals of Biomedical Engineering*, 35, 2180-2195.

[54] Tian, J.B., Ta, N., Rao, Z.S., Xu, L.F. & Huang, X.S (2013) Finite Element Modeling of Sound Transmission Based on Mirco-Computer Tomography for Human Ear, *Applied Mechanics and Materials,* 419, 593-601.

[55] Juan, Y. W., Wei, J.M. & Lin, H.B. (2011) Numerical Model on Sound-Solid Coupling in Human Ear and Study on Sound Pressure of Tympanic Membrane, *Mathematical Problems in Engineering*.

[56] Areias, B., Santos, C., Jorge, R.M.N., Gentil, F. & Parente, M.PL. (2016). Finite Element Modelling of Sound Transmission from outer to inner ear, *Journal of Engineering in Medicine,* 1-9.

List of Papers and Award

International Journal (Full paper with reviews)

1. "Finite Element Dynamics of Human Ear System Comprising Middle Ear and Cochlea in Inner Ear", Hidayat, Shingo Okamoto, Jae Hoon Lee, Naohito Hato, Hiroyuki Yamada, Daiki Takagi, *Journal of Biomedical Science and Engineering,* Vol. 6, pp.597-610, 2016.

Proceeding of International Conferences (Full paper with reviews)

1. "Dynamics Analyses of Human Middle Ear System Using Finite Element Method", Hidayat, Shingo Okamoto, Jae Hoon Lee, Kazuo Matsuura, Naohito Hato, Hiroyuki Yamada, Daiki Takagi, *Conference Proceeding of ECBA 2016 (Engineering & Technology, Computer, Basic & Applied Sciences 2016)*, Vol 127, No. 5, pp.10-21.
2. "Proper Material Properties and Dimensions of Sliced Materials used in Myringoplasty", Hidayat, Shingo Okamoto, Jae Hoon Lee, Naohito Hato, Hiroyuki Yamada, Daiki Takagi, *Proceeding of ISEAS (International Symposium and Engineering and Applied Science*). August 14-16, 2017, Osaka, Japan.

Award

1. **Best Paper Award : "**Dynamics Analyses of Human Middle Ear System Using Finite Element Method", Hidayat, Shingo Okamoto, Jae Hoon Lee, Kazuo Matsuura, Naohito Hato, Hiroyuki Yamada, Daiki Takagi, *Conference Proceeding of ECBA 2016 (Engineering & Technology, Computer, Basic & Applied Sciences 2016)*, Vol 127, No. 5, pp.10-21.

Acknowledgements

Be grateful and all glory to the Almighty God ALLAH SWT for having given a great opportunity to carry out this research. Shalawat is addressed to Rasulullah Muhammad, SAW.

Expressions of gratitude are deservedly given to Directorate General of Higher Education of Indonesia, the State Polytechnic of Samarinda and Ehime University for having given the opportunity to be a doctoral student in Robotics Laboratory of Ehime University.

Great and high appreciations are specially addressed to Prof. Shingo Okamoto for his guidance and support as my main supervisor for three years in Robotics Laboratory of Ehime University. Great and high appreciations are also addressed to Associate Prof. Jae Hoon Lee for his guidance and support as my co-supervisor and reviewer in this study. I would also like to thank the staffs of Medical Department of Ehime University, Prof. Naohito Hato as a reviewer in this study, Assistant Prof. Hiroyuki Yamada and Research Associate Daiki Takagi for their guidance and valuable input in this study. I am also grateful to Prof. Satoru Shibata and Prof. Kazunori Yasuda for their opinions and suggestions as reviewers in this study. Special thank also addressed to Altair Engineering, Ltd. for providing the license of Hyper Works by Academic Open Program (AOP).

Last but not least, I extend my deepest thank to my parents, my lovely wife, Hikmah Mujtahidah, my children, Syifa and Rashad for their endless support, care, and prayers. Finally, many thanks are expressed to all members of Robotics Laboratory of Ehime University and my friends who had supported me during the period of this study.

Curriculum Vitae

Name : Hidayat

Place/Date of Birth : Makassar, Indonesia / Mei 19, 1975

Gender : Male

Background of Education

1. Master (M.Eng) : Mechanical System Design, Mechanical Engneering, Sepuluh Nopember Institute of Technology, Indonesia (2007-2009)
2. Bachelor (B.Eng) : Energy Coversion, Mechanical Engineering, Hasanuddin University, Indonesia (1994-2000)

Occupation : Lecturer

Institution : State Polytechnic of Samarinda, Indonesia

Department : Mechanical Engineering

Study Program : Mechanical Engineering

Personal Email Address : hidayatmarlang75@gmail.com